The hydrological regime of a forested tropical Andean catchment

Kathryn E. Clark[1,2], Mark A. Torres[3], A. Joshua West[3], Robert G. Hilton[4], Mark New[5,1], Aline B. Horwath[6], Joshua B. Fisher[7], Joshua M. Rapp[8,9], Arturo Robles Caceres[10], and Yadvinder Malhi[1]

[1] Environmental Change Institute, School of Geography and the Environment, University of Oxford, Oxford, UK. (*correspondence: kathryn.clark23@gmail.com)

[2] current address: Department of Earth and Environmental Sciences, University of Pennsylvania, Philadelphia, PA, USA)

[3] Department of Earth Sciences, University of Southern California, Los Angeles, CA, USA.

[4] Department of Geography, Durham, Durham University, UK.

[5] African Climate and Development Initiative, University of Cape Town, Rondebosch, Cape Town, South Africa.

[6] Department of Plant Sciences, Cambridge, University of Cambridge, UK.

[7] Jet Propulsion Laboratory, California Institute of Technology, Pasadena, CA, USA.

[8] Department of Biology, Wake Forest University, Winston Salem, NC, USA.

[9] Current address: Department of Evolution and Ecology, University of California, Davis, CA, USA.

[10] Facultad de Ciencias Biológicas, Universidad Nacional de San Antonio Abad del Cusco, Cusco, Peru.

Abstract

The hydrology of tropical mountain catchments plays a central role in ecological function, geochemical and biogeochemical cycles, erosion and sediment production, and water supply in globally important environments. There have been few studies quantifying the seasonal and annual water budgets in the montane tropics, particularly in cloud forests. We investigated the water balance and hydrologic regime of the Kosñipata catchment (basin area 164.4 km^2) over the period 2010-2011. The catchment spans over 2500 m in elevation in the eastern Peruvian Andes and is dominated by tropical montane cloud forest with some high elevation *puna* grasslands. Catchment wide rainfall was 3112±414 mm yr^{-1}, calculated by calibrating Tropical Rainfall Measuring Mission (TRMM) 3B43 rainfall with rainfall data from 9 meteorological stations in the catchment. Cloud water input to streamflow was 316±116 mm yr^{-1} (9.2% of total inputs), calculated from an isotopic mixing model using deuterium excess (Dxs) and δD of waters. Field stream flow was measured in 2010 by recording height and calibrating to discharge. River runoff was estimated to be 2796±126 mm yr^{-1}. Actual evapotranspiration (AET) was 688±138 mm yr^{-1}, determined using the Priestley and Taylor – Jet Propulsion Laboratory (PT-JPL) model. The overall water budget was balanced within 1.6 ± 13.7 %. Relationships between monthly rainfall and river runoff follow an anti-clockwise hysteresis through the year, with a persistence of high runoff after the end of the wet season. The size of the soil- and shallow ground-water reservoir is most likely insufficient to explain sustained dry season flow. Thus, the observed hysteresis in rainfall-runoff relationships is best explained by sustained groundwater flow in the dry season, which is consistent with the water isotope results that suggest persistent wet season sources to stream flow throughout the year. These results demonstrate the importance of transient groundwater storage in stabilizing the annual hydrograph in this region of the Andes.

1. Introduction

The routing of water from the eastern flank of the Andes determines the quantity and quality of this economically and ecologically valuable resource for the region (Célleri and Feyen, 2009; Barnett et al., 2005; Postel and Thompson, 2005) and impacts the biogeochemical cycles and ecology of the lowland Amazon (McClain and Naiman, 2008; Allegre et al., 1996; Stallard and Edmond, 1983). The Amazon River has the highest discharge of all of the world's rivers, at 6300 $km^3 yr^{-1}$, with a very high runoff of 1000 mm yr^{-1} over its watershed (Milliman and Farnsworth, 2011), and it contributes 20% of the global water discharge to oceans (Beighley et al., 2009; Richey et al., 1990). The Andean portion of the Amazon Basin (> 500 m) represents an area of 623 217 km^2 and covers ~10% of the Amazon River Basin (McClain and Naiman, 2008). Although the water input from the Andes to the Amazon is approximately proportional to areal coverage (10%) (McClain and Naiman, 2008; Dunne et al., 1998), the Andes are the dominant source of the Amazon's dissolved load (McClain and Naiman, 2008; Gaillardet et al., 1999; Guyot et al., 1996), and contribute 80-90% of its suspended sediment (Richey et al., 1986; Meade et al., 1985; Gibbs, 1967) . Steep high elevation Andean slopes are a particularly important source of material delivered to the lowland Amazon (Lowman and Barros, 2014). Information about Andean river discharge, flow sources, and flow routing is thus critical for understanding the suspended sediment fluxes and chemical weathering processes of the Amazon River (Bouchez et al., 2012; Wittmann et al., 2011; Guyot et al., 1996), for quantifying how the Andes contribute to carbon and nutrient cycles (Clark et al., 2013; Townsend-Small et al., 2008), and for assessing the aquatic ecology of the region (Anderson and Maldonado-Ocampo, 2011; Ortega and Hidalgo, 2008). Hydrologic information is particularly important for understanding related responses to changes in climate and land-use.

Despite this importance, the dynamics of Andean hydrology are still incompletely characterized. This is especially true in Andean Tropical Montane Cloud Forest (TMCF), which comprises a small area (Bubb et al., 2004) but is likely to contribute disproportionately to the overall water balance of the region due to its topographic position that receives high precipitation (Bruijnzeel et al., 2011; Killeen et al., 2007). The hydrology of TMCFs is of particular interest because these forests are valuable and diverse ecosystems (Bruijnzeel et al., 2010; Bubb et al., 2004; Myers et al., 2000) and have been shown to provide an important supply of water to downstream regions, due in large part to their relatively high water yield, i.e. high stream water output for a given precipitation input (Tognetti et al., 2010; Zadroga, 1981). TMCFs are unique hydrologic systems because of the additional water input from cloud water interception (CWI) and because frequent fog occurrence may lower incoming solar radiation, increasing humidity and potentially lowering evapotranspiration (ET) (Giambelluca and Gerold, 2011; McJannet et al., 2010; Zadroga, 1981).

Transient groundwater storage may play a significant role in mountain hydrological systems (Andermann et al., 2012; Calmels et al., 2011; Tipper et al., 2006). The importance of groundwater in TMCF hydrology has recently been highlighted by studies in a Mexican TMCF, where groundwater was shown to stabilize the rainfall-runoff response (Muñoz-Villers and McDonnell, 2012), and in an Andean TMCF in Ecuador, where considering the

effect of groundwater reservoirs was important for accurately predicting streamflow (Crespo et al., 2012). Improved understanding of the extent to which groundwater stabilizes Andean TMCF hydrology is likely to be important for accurately assessing how environmental change, such as land use change or shifting cloud base, might affect hydrological functioning in the Andes and downstream in the Amazon (Rapp and Silman, 2014; Crespo et al., 2012; Bruijnzeel et al., 2011; Mulligan, 2010; Ataroff and Rada, 2000).

In this paper we evaluate stream discharge of the Kosñipata River, in a well-studied region in the eastern Andes of Peru (Rapp and Silman, 2014; Halladay et al., 2012a; van de Weg et al., 2012; Salinas et al., 2011; Girardin et al., 2010; Malhi et al., 2010), over a one-year period. We compare discharge data to rainfall, CWI, and evapotranspiration estimates in order to assess the water balance and hydrologic variability throughout the study year. We determine rainfall from meteorology station data and TRMM datasets, and we estimate actual evapotranspiration using meteorological driver data and the Priestley-Taylor Jet Propulsion Laboratory (PT-JPL) model (Fisher et al., 2008). We use the distinct water isotope composition of cloud and rain water to constrain the role of cloud water input. Stable water isotopes, i.e. δD (‰) and δ^{18}O (‰), can be used to distinguish water sources due to distinct fractionation that occurs during evaporation and condensation (Scholl et al., 2011; Froehlich et al., 2002; Gat, 1996; Rozanski et al., 1993; Craig, 1961). Stable water isotopes have been used in studies of cloud forest hydrology to deduce the contribution of wet season precipitation to dry season streamflow (Guswa et al., 2007), estimate local water recycling (Scholl et al., 2007; Rhodes et al., 2006), determine temporal and spatial variation of rainfall (Windhorst et al., 2013), trace water paths through soil layers in a catchment (Goller et al., 2005), evaluate water sources in stormflow (Muñoz-Villers and McDonnell, 2012), quantify water mean transit time (Timbe et al., 2014), and examine ecohydrological processes including seasonal water-plant relations (Goldsmith et al., 2012), and interactions between fog and vegetation (Dawson, 1998). In this study, we extend the application of stable water isotopes to constrain the contributions of different precipitation sources to annual streamflow, and in the process we add valuable new water isotope data to a growing number of TMCF studies in the Andes (Windhorst et al., 2013).

There are few similar studies evaluating the water budget in TMCF (Caballero et al., 2013; Schellekens, 2006; Zadroga, 1981), with particularly few providing comprehensive estimates of precipitation inputs (Schellekens, 2006). Our comprehensive analysis of the sources and sinks in the Kosñipata catchment allows us to focus attention on the following questions: 1) How well can the annual water budget of the Kosñipata catchment be closed and what are the uncertainties? 2) What is the importance of baseflow, i.e. the constant supply of water throughout the year, not associated with short term fluctuations due to storms? 3) Are there any significant seasonal lags between rainfall and stream runoff, and what are the causes of these lags? 4) What is the relative importance of rainfall and cloud water in sustaining streamflow throughout the year? and 5) What are the roles of soil and groundwater storage in determining seasonal patterns of river flow?

2. Study Area

The Kosñipata catchment (13°3'37" S, 71°32'40" W) study area ranges from 1360 to 4000 meters above sea level (masl) (Fig. 1a). We focus on the Kosñipata River measured at the San Pedro gauging station, which drains an area of 164.4 km^2. In the supplementary section we present results from the nested Wayqecha sub-catchment that encompasses the headwaters of the Kosñipata River, draining an area of 48.5 km^2 (Table 1). Downstream of the study region, the river flows into the Alto Madre de Dios River which feeds the Madre de Dios River (Fig. 1b), a major tributary of the Amazon River (Fig. 1c). The geology of the study area is dominated by meta-sedimentary mudstones covering ~80% of the catchment with a plutonic intrusion comprising ~20% of the catchment (Table 1) (Carlotto Caillaux et al., 1996). The geological characteristics and vegetation of the catchment are generally representative of the larger eastern Andean region of southern Peru and northern Bolivia (INGEMMET, 2013; Consbio, 2011; Carlotto Caillaux et al., 1996).

The climate of the Eastern Andes is influenced by the South American Low Level Jet (SALLJ), which carries humid winds west over Amazonia and then south along the Andean flank (Marengo et al., 2004). The Kosñipata catchment sits in a band of persistent cloudiness that runs along the Eastern Andes (Halladay et al., 2012a) and has high rainfall relative to the Andean regions to the north and to the south because of its location on an east-west kink of the Andean range that situates it perpendicular to the SALLJ (Killeen et al., 2007). Within the catchment, rainfall decreases with increasing elevation, from 5300 mm yr^{-1} at 1500 masl down to 1560 mm yr^{-1} at 3025 masl, near the treeline (Girardin et al., 2014; Huaraca Huasco et al., 2014) where down-valley winds collide with most air from Amazonia (Halladay et al., 2012a). Due to orographic effects, rainfall is highest from 1000 to 1500 masl (Rapp and Silman, 2012). Note that lower total annual rainfall amounts were reported previously for this catchment (Lambs et al., 2012), but the data used in this previous study were incomplete for the locations where we recorded highest rainfall. Orographic fog (cf. Scholl et al. (2011)) plays an important role in the Kosñipata catchment. Cloud base varies in height throughout the year, with the cloud base at its lowest in the dry season (June to August) (Halladay, 2011). In July (mid-dry season) the cloud base is >60% of the time >1800 masl and 30% of the time between 1500-1800 masl (Rapp and Silman, 2014). Nearby, in the Central Peruvian Andes on leeward slopes, intercepted evaporation (rainfall interception losses by the canopy) was 210 mm yr^{-1} in the UMCF and 660 mm yr^{-1} in the LMCF (Gomez-Peralta et al., 2008); similar ranges are expected in the Kosñipata catchment. Annual mean temperatures in the Kosñipata catchment range from ~19 °C at low elevations to ~12 °C at high elevations (Girardin et al., 2014; Huaraca Huasco et al., 2014) with an adiabatic air temperature lapse rate of 4.94 °C km^{-1} of altitude (Girardin et al., 2010). The wet season is generally defined to be December to March, the wet-dry transition season to be April, the dry season to be May to September, and the dry-wet transition season to be October and November (Table S1). These terms are used in a relative sense in the Andes, since precipitation is still significant in the dry season.

Cloud water interception has not been measured previously in this part of the Andes, but in other similar TMCFs, CWI ranges from 50 to 1200 mm yr^{-1} (Bruijnzeel et al., 2011). In many perhumid TMCFs (Holwerda et al., 2010a; Holwerda et al., 2010b; McJannet et al.,

2010; Schmid et al., 2010; McJannet et al., 2007; Eugster et al., 2006), CWI typically makes up a smaller proportion of the total input compared to seasonal and drier areas where CWI is often a more important component in the annual water budget (García-Santos and Bruijnzeel, 2011; Marzol-Jaén et al., 2010; Guswa et al., 2007; Mulligan and Burke, 2005).

The Kosñipata catchment is dominated by forest (~93%) with the remainder of the area covered by high elevation grasslands called *puna* (Squeo et al., 2006) (Table 1) (Consbio, 2011). The timberline, the lowest elevation at which trees do not grow, occurs at 3000 to 3600 masl with *puna* grasslands and shrubland at higher elevations (Gibbon et al., 2010). The soils in the *puna* grasslands are usually saturated for ~8 months of the year (November to June; I. Oliveras personal communication, 2013) due to relatively high precipitation and low temperatures (Wilcox et al., 1988). Small areas of bare bedrock are exposed at the highest elevations. In the forested area of the Kosñipata catchment, vegetation consists of upper montane cloud forest from approximately 2000 to 3450 masl, and lower montane cloud forest and lower montane tropical rainforest from approximately 1200 to 2000 masl (Consbio, 2011). The Kosñipata catchment is partially contained in Manu National Park, where logging is prohibited. The soils in the forested parts of the catchment are predominantly inceptisols (Asner et al., 2014). Soil water content varies temporally by < 15% throughout the year and soil moisture ranges spatially from 21 to 71 % throughout the catchment (Girardin et al., 2014; Huaraca Huasco et al., 2014; Teh et al., 2014). At lower altitudes there are only short periods at mid-day at the driest time of year which show some signs of moisture stress (Rapp and Silman, 2012).

3. Materials and Methods

3.1. Catchment wide rainfall estimates

Meteorological stations are located throughout the Kosñipata valley along an altitudinal gradient from 887 to 3460 masl (Fig. 1a & 2a), distributed in various landcover types and on a range of slopes and aspects (Table S2). Only data from the Wayqecha meteorological station (at 2900 masl) were recorded over the full length of this river study, so rainfall was estimated using the long-term monthly record from 0.25° × 0.25° merged Tropical Rainfall Measuring Mission (TRMM) data (TRMM, 2013) together with the long-term monthly rainfall data from nine meteorological stations (Girardin et al., 2014; Huaraca Huasco et al., 2014; ACCA, 2012; Rapp and Silman, 2012; SENAMHI, 2012).

The 3B43 v7a TRMM is a third level product with outputs in mm d^{-1}, which have been converted to mm $month^{-1}$ with an output each month from 1998 to 2012. The Kosñipata catchment is situated entirely within one 3B43 TRMM tile, which covers an area of ~730 km^2 centred at 12°7'48"S, 71°38'6"W (Fig. 1a). The raw TRMM 3B43 data underestimates rainfall in the Andes (Scheel et al., 2011; Bookhagen and Strecker, 2008). Indeed, in the case of the Kosñipata catchment, TRMM 3B43 rainfall is an underestimate compared to nearly all of the data from meteorological station rainfall gauges in the catchment and is most comparable to the meteorological stations at high elevations with low rainfall (Fig. 2a).

Because of the apparent systematic bias, we did not use the TRMM data directly but instead calibrated the TRMM data using meteorological data to make catchment wide rainfall estimates. This had the advantage of allowing us to use the long-term TRMM record that covers periods of time when data is not available from the meteorological stations, since the latter only have sporadic coverage, ranging from 13 to 79 months (Table S2). Details of the calibration procedure we used are provided in the supplementary section.

In order to make robust catchment wide rainfall estimates, rainfall loss due to wind around the rainfall gauge was estimated using wind data from available meteorological stations along the Trocha Union ("Union Trail") at 3450, 2750, and 1800 masl and at San Pedro at 1500 masl (Table S2). Cup anemometers were located in the tree canopy at the same height as the rain gauges. Correction of rainfall using wind speed followed Equations 1 and 2 in Holwerda et al. (2006). The mean and standard error of wind speed and wind-induced rainfall loss (%) were determined seasonally and annually (Table S3), and seasonal averages for wind-loss rainfall (%) were used to correct catchment wide rainfall (corresponding to an annual correction of 2.50±0.56%).This approach may underestimate some wind-loss rainfall since the correction may have been larger at some meteorological stations (e.g., 4.2% at Wayqecha), but precise wind data were only available at a few sites so it was not possible to make site-specific corrections for all of the rainfall data from individual meteorological stations.

3.2. Discharge and runoff measures

This study is based on measurements of Kosñipata River discharge made over a one-year period (Fig. 1a & 3), focusing on the Kosñipata River gauging station located at San Pedro (13°3'37"S, 71°32'40"W), at 1360 masl. Field measurements consisted of river height, flow velocity, and cross-sectional area, which together allowed us to estimate discharge and runoff over the study period. For full details of the measurements and corrections see the supplementary section; a brief summary is provided here. River stage height was measured from January 2010 to February 2011 using a river logger (Global Water WL16 Data Logger, range 0- 9 m), recording river level every ~15 min. The instantaneous discharge associated with each height measurement was calculated based on calibrated stage-discharge relationships. Total monthly discharge was determined by summing over each month, and the monthly totals were converted into an instantaneous discharge ($m^3 s^{-1}$) for each month. Monthly, seasonal and annual discharge and runoff were determined from these values. There was a gap in the logger data of 31 days in the dry season between mid-July and early-August (Fig. 3); these gaps were filled by linear interpolation. This interpolation misses storms, but these should have little influence on the annual discharge because of low flow throughout this period of time. Baseflow was determined from mean daily discharge ($m^3 s^{-1}$) using the method outlined in Gustard et al. (1992). Base flow index (BFI) was calculated as the ratio of the total volume of baseflow divided by the total volume of streamflow.

3.3. Actual evapotranspiration estimates

Actual evapotranspiration (AET) was estimated using the ecophysiologically downscaled PT-JPL (Priestley and Taylor – Jet Propulsion Laboratory) AET method developed by Fisher et al. (2008). This method has been evaluated extensively throughout the tropics (Fisher et al., 2009). The model is based on ecophysiological theory using traits that are measurable in the field or remotely. It takes a bio-meteorological approach incorporating the radiation based model from Priestley and Taylor (1972) to determine rates of actual evapotranspiration. The model requires only four variables: normalised difference vegetation index (NDVI), net radiation (R_n), maximum air temperature (T_{max}), and minimum relative humidity (RH_{min}). The PT-JPL model predicts three components of the evapotranspiration budget: canopy transpiration (AET_c), rainfall evaporation interception (AET_i), and soil evaporation (AET_s). Details of the parameter values selected for actual evapotranspiration estimates are provided in the supplementary section.

3.4. Water isotope measurements

River water, rainfall, and cloud water were collected from 2009 to 2011 from a range of elevations throughout the catchment. River water was collected from the river surface, passed through a 0.2 μm nylon filter, and stored unpreserved in containers that prevented evaporative loss (see supplement). Rainfall samples were collected at the time of river water collection near the river gauge, with additional samples collected along an altitudinal transect in the catchment between 1500 to 3600 masl (Table S4a). Cloud vapour was collected along the altitudinal transect below the canopy using a cryogenic pump (Table S4b).

Isotopic analysis was carried out on the samples to determine δD (delta deuterium, $^2H/^1H$, ‰), $\delta^{18}O$ (delta 18-oxygen, $^{18}O/^{16}O$, ‰) and deuterium excess (defined as $Dxs = \delta D - 8 \times \delta^{18}O$, in ‰), all reported to relative to Standard Mean Oceanic Water (SMOW). Deuterium excess (Dxs), representing the offset from the meteoric water line (see supplement), provides information about the source conditions of water vapour (Dansgaard, 1964). It is controlled by kinetic effects during evaporation, where a larger Dxs value is an indicator of enhanced moisture recycling and a lower value indicates an enhanced evaporative loss (Cappa et al., 2003; Salati et al., 1979).

River water, rainfall, and water vapour samples were analysed with a Picarro L1102-i cavity ring down spectrometer (CRDS). River water and rainfall from 2011 were injected 5 times and the final 3 samples averaged. Precision (1σ) was 0.2‰ for $\delta^{18}O$ and 1‰ for δD, though some samples showed larger uncertainties. VSMOW and VSLAP standards were analysed at the same time and were used to assess accuracy and precision of the instrument between runs. Rainfall from 2009 and water vapour were injected 9 times and the final 6 samples averaged. Precision (1σ) was <0.1‰ for $\delta^{18}O$ and 1‰ for δD. Calibration of results to VSMOW was achieved by analysing internal standards before and after each set of 7 to 8 samples. Internal standards SPIT, BOTTY, and DELTA were used to calibrate against VSMOW. Additional analyses using Isotope Radio Mass Spectrometry (IRMS) were used as a check on the CRDS results (see supplement).

4. Results

4.1. Catchment wide rainfall

The estimated annual wind-loss corrected rainfall for the 12-month study period (February 2010 to January 2011) was 3112 ± 414 mm, or 90.8 ± 16.5 % of total water inputs (3428 ± 430 mm) (Table 2), where uncertainties are propagated errors reported at one standard deviation (the same convention is used throughout the text). Based on the long-term calibrated TRMM record, the 15-year (1998 to 2012) mean annual rainfall was 2881±124 mm, indicating that our river discharge measurements were made in a year with slightly higher than average rainfall (Fig. 4; Table S5). The total rainfall contribution over the study period was divided into 100 m altitudinal bins to evaluate how rainfall was distributed over the catchment. Although most of the catchment area is located at mid to high elevation ranges (~2400-3400 masl), maximum rainfall occurs at ~2400 masl (Fig. 2c).

4.2. Discharge and Runoff

The Kosñipata River basin at San Pedro, with a mean elevation of 2805 masl and an area of 164.4 km^2, was estimated to have a mean discharge of 14.6±0.7 $m^3 s^{-1}$ and runoff of 2796±126 mm (81.6 ± 11.0 % of total precipitation) over the 1-year study period (Table 2). This value falls within the runoff range of 2100 to 3070 mm yr^{-1} for 2 microcatchments in the Ecuadorian Andes, with very similar vegetation cover and elevation (Crespo et al., 2011). In the Kosñipata catchment, 52% of the annual flow was during the wet season, which covers only 33% of the year (Table 2).

Baseflow was 2173±133 mm of the annual total runoff. The base flow index (BFI) is the ratio between the total baseflow volume and total streamflow volume. The BFI value for the Kosñipata (77%) is consistent with the 2 Ecuadorian catchments discussed above, where 80% of annual flow was attributed to baseflow (Crespo et al., 2011).

4.3. Evapotranspiration

Actual evapotranspiration (AET) was estimated from the PT-JPL model (Fisher et al., 2008) at 688±138 mm (20.1 ± 4.8 % of total precipitation). In previous work in lowland tropical forests, AET was estimated to be 1000-1300 mm yr^{-1} (Bruijnzeel et al., 2011; Fisher et al., 2009), while TMCFs were characterised by ET values more similar to the Kosñipata catchment, between 545 and 1200 mm yr^{-1} (Bruijnzeel et al., 2011). AET in TMCFs is reduced because fog immersion in TMCFs reduces solar radiation and lowers the vapour pressure deficit, resulting in lower atmospheric evaporative demand (McJannet et al., 2010; Letts and Mulligan, 2005; Bruijnzeel and Veneklaas, 1998), and because wet leaf surfaces lower transpiration and photosynthesis (Letts and Mulligan, 2005).

The Interception evaporation component of the PT-JPL model was not tested against data because no data were available. However, the model has been tested against many lowland tropical forest flux sites, where the total ET measured does include intercepted evaporation (Fisher et al., 2008). In the Kosñipata catchment the PT-JPL model predicts

intercepted evaporation to be 226±45 mm yr^{-1} in the UMCF, 324 ± 65 mm yr^{-1} in the LMCF, and 104 ± 21 mm yr^{-1} in the puna/transition. This compares favourably with direct intercepted evaporation estimated in the Yanchaga-Chemillen forests in the central Peruvian Andes, where intercepted evaporation in UMCF contributed 210 mm yr^{-1} or 7.7% of the bulk precipitation, and in LMCF it contributed 660 mm yr^{-1} or 33% of the bulk precipitation input (Gomez-Peralta et al., 2008). Our basin-wide estimate of AET_i was 225 ± 45 mm yr^{-1} or 6.6 ± 1.6 % of the bulk precipitation (3428 ± 430 mm yr^{-1}).

Sap flow was measured in tree trunks in the Wayqecha forest plot (2900 masl) for one month from mid-July to mid-August 2008. These sap flow values were used in the soil-plant atmospheric (SPA) model to predict a canopy transpiration rate of 53 mm $month^{-1}$ (van de Weg et al., 2014). For the same time period, using the same meteorological data, the PT-JPL model predicted a canopy transpiration (AET_c) of 49 mm. These similarities suggest that even though the PT-JPL model has not been deployed in TMCF previously, it provides a reasonable estimate of canopy transpiration and intercepted evapotranspiration. Thus, we allocate a maximum error of ~20% on AET.

4.4. Isotopic analyses and mixing calculations

Rainwater δD and $\delta^{18}O$ values display considerable seasonal variation whereas variation with elevation during a given season is less pronounced (Table S4a; Fig. 5). Rainwater δD and $\delta^{18}O$ values are highest during the dry season. Seasonal variation in Dxs is minimal (Fig. 5). The $\delta^{18}O$ and δD of Kosñipata cloud water vapours are not clearly distinct from rainwaters. This result departs from the isotopic enrichment found in cloud waters in non-orographic settings, but similarity between cloud and rainwater isotopes has also been found in the few cases of orographic cloud formation that have been studied (Scholl et al., 2011). Despite the overlap in $\delta^{18}O$ and δD, the cloud water vapour samples from the Kosñipata catchment have higher and more variable Dxs values than all of the rainwater samples (Fig. 5; Table S4b).

Streamwater δD, $\delta^{18}O$ and Dxs values ranged from -94.8 to -64.9 ‰, -14.5 to -10.9 ‰, and 19.1 to 22.6 ‰ respectively (Table S6). A slight seasonality is apparent in stream water isotopic composition, with slightly higher δD values during the dry season and dry-to-wet season transition (Fig. 6a). A significant seasonal variation in Dxs in streamwater is not apparent (Fig. 6b). See the supplementary section for full details on the δD, $\delta^{18}O$, and Dxs isotope results.

Qualitative comparison between the Kosñipata River water isotope data and the rainwater and cloud water isotope data suggests that, throughout the year, wet season precipitation is the dominant contributor to river discharge (Fig. 5). As discussed below, this probably results from the storage of wet season precipitation in groundwater that is released to the stream over time. It is possible that isotopic enrichment may take place via evaporation as water makes its way from precipitation to streamflow, either associated with throughfall (e.g. Brodersen et al. (2000)) or in soils (e.g. Dawson and Ehleringer (1998); Thorburn et al. (1993)). Such isotopic enrichment could bias inferences about water sources using isotopic

signatures. However, we note that any evaporative enrichment would act to decrease the relative contribution from wet season rainfall (the depleted source), supporting the qualitative inference that wet season rainfall is the dominant source of streamflow throughout the year. Moreover, the Kosñipata streamwaters appear to have little geochemical imprint of evaporation. Chloride concentrations provide a conservative tracer that should be enriched during evaporation; in the Kosñipata samples, Cl concentrations are similar in rainwater (2-20 μM) and streamwater (2-12 μM) (Torres et al., in review). Kosñipata stream waters also lie on the same local meteoric water line as rainwater (see Supplement), with no evidence for relative D-depletion that may be expected during evaporation.

To quantitatively constrain the relative contributions of different water sources to river discharge, a three end-member mixing model was used (see supplementary info for details). In this model, mixing between wet season precipitation, dry season precipitation, and dry season cloud water vapour is considered along with observed variability in the isotopic compositions of each of these end-members (i.e. Phillips and Gregg (2001)). Since we assume minimal evaporative enrichment of water isotopes during runoff generation, the results of this model provide a minimum constraint on the contribution from wet season rainfall. Results of the three end-member mixing calculations are distributions of possible end-member contributions (Fig. 6c to f). For individual samples, mean contributions of wet season rainfall, dry season rainfall, and cloud water vapour to river discharge range from 46-67%, 19-33%, and 7-31% respectively (Fig. 6f; Table S7). Similarly, the maximum likely contributions of each source to a single sample, which we define as the 95^{th} percentile value of the distributions from our mixing calculations, range from 66-87%, 38-60%, and 19-52% for wet season precipitation, dry season precipitation, and cloud water vapour respectively (Fig. 6c to f). It is worth noting that only two samples (n = 62) show mean and maximum likely contributions of cloud water vapour greater than 18% and 40% respectively (Fig. 6f; Table S7). These contributions calculated from the water isotope mixing model reflect the ultimate source of the water to stream runoff, with storage and mixing in groundwater likely to be an important intermediary but one which would not affect the source partitioning.

4.5. Cloud water in streamflow

Isotopic mixing calculations constrain the statistically most likely cloud water vapour contribution to between 7 and 31% of streamflow, with only 2 samples >18% (Table S7). All samples, except for the two with the highest analytical uncertainties, show this range of cloud water vapour contribution regardless of collection season (Figs. 6f and 7c). Based on our estimated monthly total river discharge and the average values for cloud water contribution in each month, we estimate that total cloud water contribution to streamflow was 316±116 mm yr^{-1}, using the 50^{th} percentile values of the cloud water fraction and confidence intervals defined by the 5^{th} and 95^{th} percentiles (Tables 3 & S7). Our estimated cloud water flux to the river falls within the (admittedly very broad) range of CW interception fluxes measured in TMCFs, which range from ~50 to 1200 mm yr^{-1} (Bruijnzeel et al., 2011; Bendix et al., 2008). Compared to our annual discharge of 2796±126 mm, this means cloud water contributed 11±4% to annual streamflow.

Our results suggest that cloud water appears to play a non-negligible contribution to stream runoff in the Kosñipata River, but that it remains secondary to precipitation inputs even during the dry season when rainfall is at its lowest and cloud immersion is most frequent. Cloud frequency is high in the catchment, with cloud cover > 70% year round (Halladay et al., 2012a). In the dry season the cloud base was > 1800 masl 40% of the time (Rapp and Silman, 2014). Cloud immersion is a key characteristic of tropical montane cloud forest (Bruijnzeel et al., 2011), and provides an important water source to the forest canopy and the diverse epiphyte community (Rapp and Silman, 2014; Bruijnzeel et al., 2011; Giambelluca and Gerold, 2011). However, it is possible that much of the intercepted water is transpired or evaporated directly from the canopy. Overall, cloud water contribution to stream runoff supplies a relatively constant proportion of total flow throughout the year and never dominates water inputs to the Kosñipata River, even during times of the lowest flow (Table 3).

5. Discussion

5.1. Water balance

The annual water balance for the Kosñipata catchment can be described by the following equation (water inputs to the catchment on the left, losses from the catchment on the right):

$$Rainfall + CWI = AET + Runoff + Residual \quad (1)$$

Rainfall was estimated catchment-wide from TRMM and meteorological station rainfall at 3112 ± 414 mm yr^{-1}. Cloud water interception (CWI) was estimated from the isotope mixing model at 316 ± 116 mm yr^{-1}. Actual evapotranspiration (AET) was estimated from the PT-JPL model (Fisher et al., 2008) at 688 ±138 mm yr^{-1}. Runoff was estimated from the gauging station at 2796±126 mm yr^{-1} (Fig. 8a). The residual of Eq (1) sums to -56±469 mm, which is -1.6±13.4% of total annual water inputs through rainfall and CWI, indicating that any imbalance within our budget is within the estimated uncertainties of the water balance calculation.

There are several additional structural uncertainties in our calculation of the water balance for the Kosñipata catchment. Rainfall was estimated for the catchment by calibrating TRMM rainfall using actual rainfall collected from 9 gauging stations. In the Kosñipata catchment there was a decrease of rainfall with an increase of elevation, corresponding to an average annual rainfall gradient of ~ -148 mm per hundred metres (Fig. 2a). It is possible that rainfall deviates from this trend along the altitudinal gradient because our results are limited to 9 meteorological stations dispersed over a large area (Fig. 1a). Intense localised storm activity also increases the chance of underestimating precipitation. The types of rain gauges used in the catchment (Table S2) are not ideal for cloud forests due to an underestimation of wind driven precipitation on steep slopes (Bruijnzeel et al., 2011; Frumau et al., 2011). Although we have corrected for wind losses (Holwerda et al., 2006), this correction method

has not been tested specifically in the Kosñipata catchment. Stream runoff can be overestimated in mountain rivers due to an overestimation of velocity by taking measurements predominantly near the surface of the channel (Chen and Chiu, 2004; Thome and Zevenbergen, 1985). We have taken this under consideration and corrected surface velocity to estimate mean channel velocity (following Eq S1 in the Supplement), but it is possible that our runoff values remain overestimated. Taking these methodological uncertainties into consideration, our rainfall input value may be conservative, and stream runoff output value may be an upper bound.

Improvements in our estimates of the water budget might be possible from additional work including: (1) characterising the interactions between topography, wind speed and the amounts of rainfall received on slopes with varying wind exposure; 2) measuring throughfall (crown drip) stable water isotope composition, which would make it possible to use isotope mass balance of different precipitation sources to test the calculated cloud water inputs, and 3) using distinct two component mass balance models to infer CWI for the different ecosystem types (puna/transition, UMCF and LMCF), i.e., as a variant of the wet canopy water budget approach of Holwerda et al. (2006) that was also used in Scholl et al. (2011).

5.2. Hysteresis

5.2.1. Characterizing hysteresis

A monthly breakdown of the water balance shows the distribution of annual residual when water is going into storage (+) and when water is coming out of storage (– ; Fig. 9). The mid-wet season (January & February) was a time of recharge with positive residual values. This store was subsequently drained as discharge to stream runoff in the wet-dry transitional season (April) and most of the dry season (May to August), both of which showed negative residual values (Fig. 9). This seasonal shift (see Fig. 8) illustrates how rainfall stored during the wet season plays an important role in sustaining steady dry season runoff. The results of the isotope mixing analysis confirm this inference by showing that wet season rainfall is still prominent in contributing to streamflow in the dry season. Sources of streamflow from May to September 2010 were 61±9% from wet season rainfall, 25±9% from dry season rainfall, and 12±7% from cloud water (Table 3).

At seasonal timescales, streamflow and baseflow in the Kosñipata catchment both follow an annual anti-clockwise hysteresis pattern (Fig. 10). This pattern is similar to that observed by Andermann et al. (2012) in the Nepalese Himalaya. In the wet season (December to March), the catchment wide rainfall in the Kosñipata catchment was greater than streamflow and baseflow (Fig. 10a & c). During the wet-dry transition season (April), and the start of the dry season (May and June) however, there was a switch and streamflow and baseflow were greater than rainfall. By the middle of the dry season (July and August) rainfall was equal to streamflow and baseflow. By the time of the late dry season (September), rainfall started to increase and was greater than streamflow and baseflow. The dry-wet transition season (October and November) had higher rainfall than streamflow and baseflow. Finally, in the early wet season (December to January) the cycle was completed

where the contribution of rainfall dominated streamflow and baseflow (Fig. 10a & c). The annual anti-clockwise hysteresis was even more pronounced when streamflow and baseflow were compared to the rainfall gathered over the study period at the Wayqecha meteorological station at 2900 masl (Fig. 10b & d).

The water isotope data support the indication of seasonal hysteresis observed in the water balance estimates. The relationship between river discharge and δD showed a seasonal clockwise hysteresis, but this was not observed in Dxs (Fig. 7a & b). Considering the observed end-member δD and Dxs compositions, this observation implies that there was seasonal variation in the relative contributions of wet and dry season rainfall but not cloud water vapour (Fig. 7c to e). The Monte-Carlo derived confidence intervals on the mixing results provide large ranges. However, the mean results (Fig. 7), which best represent each end-member composition, show a seasonal anti-clockwise hysteresis between river discharge and the mean contribution of wet-season precipitation that is consistent with the hysteresis observed in the water balance. Dry season and dry-wet transitional season runoff appear to be sustained by relatively lower, but still dominant, contributions from wet season precipitation (Fig. 7d). A corresponding variation in the contribution of dry season precipitation with discharge is also evident, whereby dry season and dry-wet transitional season runoff is composed of a larger proportion of dry season rainfall (Fig. 7e). The hysteresis in the mixing model results is attributable to the seasonal hysteresis in streamwater δD. No seasonal hysteresis in the contribution of cloud water interception to river discharge is apparent (Fig. 7c), consistent with no seasonal pattern in the streamwater Dxs.

The consistent, annual anti-clockwise hystereses in both the water balance and the contribution from different sources inferred from the water isotopes indicate that there are important factors other than the storm runoff response that influenced hydrologic variability throughout the year in the Kosñipata catchment. The lag in runoff can be explained by a significant portion of wet season rainfall being stored, and then several months later discharged as runoff in the wet-dry transition and dry seasons (Fig. 10a & Table 2). The delay in rainfall to streamflow runoff helps provide water in the catchment at times of lower rainfall, stabilising dry season runoff.

5.2.2. Can soil water explain seasonal hysteresis?

There are several potential mechanisms causing a seasonal lag in streamflow. The water isotope data points to rainfall, rather than cloud water, as the primary source of water, but it is still unclear how rainfall is stored temporarily over the year. Shallow groundwater (i.e., lateral flow through soil layers) derived from accumulation of water in soils during the wet season may contribute to the delayed stream runoff. In the Kosñipata catchment, shallow groundwater may be sourced from drainage of saturated *puna* grassland soils. In *páramo* wetlands (a wetter mountain top biome) in the northern Andes of Ecuador, delayed groundwater has been shown to play an important role in dry season runoff (Buytaert and Beven, 2011). Tropical montane cloud forest soils, as found in a similar forest in Ecuador, can also be a potential source for delayed runoff over shorter periods of ~3.5 to ~9 weeks (Timbe et al., 2014).

If seasonal variations in soil water content are sufficient to account for the seasonal lag in runoff in the Kosñipata, then:

$$A_{catchment} \times ED = A_{storage} \times d \times \Delta V \quad (2)$$

where $A_{catchment}$ is the area of the drainage basin (m^2), *ED* is the seasonal excess discharge (mm) consisting of the sum of the monthly residual values from the wet-dry transitional season and most of the dry season (April to August; Fig. 9), $A_{storage}$ is the area of the basin covered in soil (m^2), d is depth of soil layer (m), and ΔV is the seasonal variation in soil water content that needs to occur to account for the excess discharge. Since the area of the catchment and area covered in soil are approximately the same, the area variables in Eq (2) cancel out. For our calculation, we assume mean soil depth (*d*) to be ~0.5 m, consistent with data from the Kosñipata catchment (Gibbon et al., 2010; Zimmermann et al., 2009). Typical soil water content in the TMCF and puna ranges spatially between 32 and 71 % (Teh et al., 2014). Catchment wide seasonal variation (ΔV) of < ~13% was estimated using basin proportions (Fig. 2c) for each ecosystem type and soil moisture variations observed in each ecosystem. LMCF/LMRF dominates from 1350 to 2000 masl and comprises 8.3 % of the catchment area, UMCF dominates from 2000 to 3450 masl and comprises 80.6% of the catchment, and transition/puna is found >3450 masl, comprising 10.1 % of the catchment (Consbio, 2011). Temporal variability in soil moisture determined in past studies (Girardin et al., 2014; Huaraca Huasco et al., 2014; Teh et al., 2014) indicates ΔV = 5.4% for LMCF/LMRF, ΔV = 15% for UMCF and ΔV = 0.4% for puna grasslands.

Using an inferred catchment-wide ΔV = 12.6%, the total discharge contributed by soil water release, i.e. the right hand side of Eq (2), is estimated to be 65 mm. This suggests that water release from soil accounts for ~17% of the total seasonal ED in the Kosñipata river, with the remaining 310 mm (83%) not explained by seasonal storage and drainage of soils. How much more variable would soil water content have to be in order to explain all of the seasonal ED? By re-arranging Eq (2) as $\Delta V = ED/d$, we find that volumetric water content would need to vary by ~75% between seasons to fully account for our calculated seasonal excess discharge of 373 mm. This magnitude of required seasonal change is much greater than observed in any of the Kosñipata soils.

5.2.3. Importance of groundwater in hysteresis

If soil water content changes are insufficient to account for the excess dry season discharge, the source of this excess discharge is likely to be groundwater stored within the fractured bedrock below the shallow soil layer. In central eastern Mexico, groundwater in the TMCF was found to be an important component of dry season runoff (Muñoz-Villers et al., 2012). Groundwater occurs mostly in permeable bedrock and within fractures of impermeable bedrock (Jardine et al., 1999; Gascoyne and Kamineni, 1994; Todd and Mays, 1980). In the Nepal Himalayas, deep groundwater recharges through fractured bedrock containing aquifers several tens of meters deep and has a storage residence time of ~45 days (Andermann et al., 2012). Fracturing and the exposure of bedding planes through the process of uplift and erosion in the Kosñipata catchment (Carlotto Caillaux et al., 1996) could provide

conduits that aid in deep groundwater flow. In the Kosñipata, ~80% of the catchment area consists of sedimentary mudstones and shale, and ~20% consists of plutonic intrusions (Table 1). Shale has a very low porosity and permeability (Domenico and Schwartz, 1998; Morris and Johnson, 1967), but when fractured its porosity is greatly increased (Jardine et al., 1999). Plutonic intrusions, as found in lower parts of the catchment, also have increased porosity as a result of fracturing (Gascoyne and Kamineni, 1994). Thus we view deep fractured bedrock as the likely transient storage reservoir that may explain the annual hydrograph in the catchment. Further investigations into the hydrogeological characteristics of the soil profile and weathered bedrock, such as saturated hydraulic conductivity (Kim et al., 2014; Kuntz et al., 2011; Larsen, 2000) and specific yields of fractured rock types (Domenico and Schwartz, 1998) would help better elucidate the role of groundwater in sustained dry season baseflow. Some of the seasonal storage of water could also be in valley fills, lower slope colluvial deposits, peat and epiphyte biomass in the TMCF, and in saprolite, and better constraining the potential water storage in such reservoirs would also be valuable further work.

The observation of a significant role for seasonal groundwater storage and release in Kosñipata River has implications for understanding Andean water resources, predicting flooding, and quantifying biogeochemical fluxes. The capacity for transient storage of water in bedrock may be affected by land use changes, particularly if forests are removed and resulting loss of forest soils reduces the "forest sponge" that facilitates water infiltration and groundwater storage during the wet season (Bruijnzeel, 2004). Our observations are important for assessing how the hydrologic system may respond to changing climate. The rate of warming over the next 100 years in the region of the Kosñipata catchment is expected to proceed an order of magnitude faster than the 1°C increase in temperature per 1000 years during the Pleistocene-Holocene (Bush et al., 2004). The observation of upslope shift of plant distributions already indicates a dramatic pace of change in the Kosñipata (Tovar et al., 2013; Feeley et al., 2011; Hillyer and Silman, 2010). It remains unclear how patterns of rainfall and cloud frequency have been changing and will change in the future (Halladay et al., 2012b; Rapp and Silman, 2012), much less how the hydrologic system will respond, both to changes in magnitude and in seasonality of precipitation sources. The baseline of water isotope data, the partitioning of precipitation sources, and the conceptual framework presented in this study offer the potential to help understand what hydrologic responses might be expected if precipitation changes (e.g. as evaluated in Puerto Rico; (Scholl and Murphy, 2014)). Moreover, further exploration and verification of the observations in this study, for example by conducting long-term streamflow measurements (Larsen, 2000), considering longer-term water budgets (Andermann et al., 2012), detailed analysis of stream hydrochemistry (Calmels et al., 2011; Tipper et al., 2006), and/or analysing the isotopic composition of throughfall (i.e. net precipitation), would strengthen understanding of how Andean TMCFs function hydrologically today and how this function may evolve in the future.

6. Conclusions

An annual water budget for the Kosñipata catchment indicates that 3112±414 mm (90.8±16.5% of total water inputs) was contributed to the catchment by rainfall, 316±116 mm (9.2 ± 3.6 % of total water inputs) was supplied by cloud water, 2796±126 mm (81.6 ± 11.0 % of total water inputs) was removed as streamflow, and 688±138 mm (20.1 ± 4.8 % of total water inputs) was lost through actual evapotranspiration. The annual water budget balances at -1.6 ± 13.4 %. Annual stream runoff was composed of 60±5 % wet season rainfall, 26±5 % dry season rainfall, and 11±4 % cloud water. Baseflow contributed 77% of the streamflow over the one year of study. Runoff followed an annual anti-clockwise hysteresis with respect to rainfall, exhibiting a lag in stream runoff that maintained stream water flow in the early dry season. 61±9 % of dry season runoff originated as wet season rainfall. The contribution from cloud water, although important to the TMCF ecology, plays a secondary role in river streamflow (~10%) in this catchment, even during the low flow of the dry season. Seasonal excess discharge measured throughout the wet-dry transitional season and dry season (April to August) was ~373 mm, with storage and release of water in soil accounting for only ~17 % of this excess. Deep groundwater in fractured rock is probably the cause of the remaining majority of the seasonal lag in stream runoff. The observation of seasonal groundwater storage in this system has important implications for how land use and climate changes may affect the hydrologic system in the Andes. Although significant over seasonal timescales, there is no evidence for significant change in groundwater storage over the course of the one year study period, given the balanced water budget and similar discharge and the beginning and end of the study.

Author contribution

KEC, AJW, RGH, MN, and YM designed the study; KEC, ARC, ABH, and JMR carried out the field work; KEC carried out data analysis; MAT analysed the water samples, developed the mixing model and carried out the streamflow source simulations; and JBF developed the PT-AET model. KEC and AJW prepared the manuscript with contributions from all the co-authors.

Acknowledgements

This paper is a product of the Andes Biodiversity and Ecosystems Research Group (ABERG). KEC was funded by the Natural Sciences and Engineering Research Council of Canada (NSERC; 362718-2008 PGS-D3) and Clarendon Fund PhD scholarships. AJW is supported to work in the Kosñipata by National Science Foundation (NSF) EAR 1227192. YM is supported by the Jackson Foundation and by European Research Council Advanced Investigator Grant 321121. We thank SERNANP for providing permits to work in the study area. We thank ACCA Peru (Wayqecha) and Incaterra (San Pedro) for field support; L.V. Morales, R.J. Abarca Martínez, M.H. Yucra Hurtado, R. Paja Yurca, J. A. Gibaja Lopez, I. Cuba Torres, J. Huamán Ovalle, A. Alfaro-Tapia, R. Butrón Loayza, J. Farfan Flores, D. Ocampo, and D. Oviedo Licona for field assistance; J. Silva-Espejo and W. Huaraca Huasco

for collection and provision of meteorological data, and SENHAMI for provision of national weather station data. We thank L. Anderson for the TRMM 3B43 v7a data; C. Girardin for assistance with the water budget figure; S. Abele for extraction of the SENAMHI rainfall data; M. Palace for the 2009 Quickbird image; G.P. Asner for use of the Carnegie Airborne Observatory (CAO) DEM; S. Waldron, S. Feakins and G. Goldsmith for constructive comments and discussions; L. A. Bruijnzeel and M. B. Gush for their thorough and constructive reviews; G. Jewitt for editing the manuscript.

References

ACCA: Weather data San Pedro station, Asociación para la concervación de la cuenca Amazónica http://atrium.andesamazon.org/index.php, (last access: April 2012), 2012.

Allegre, C. J., Dupre, B., Negrel, P., and Gaillardet, J.: Sr-Nd-Pb isotope systematics in Amazon and Congo River systems: Constraints about erosion processes, Chem. Geol., 131, 93-112, http://dx.doi.org/10.1016/0009-2541(96)00028-9, 1996.

Andermann, C., Longuevergne, L., Bonnet, S., Crave, A., Davy, P., and Gloaguen, R.: Impact of transient groundwater storage on the discharge of Himalayan rivers, Nat. Geosci., 5, 127-132, http://dx.doi.org/10.1038/NGEO1356, 2012.

Anderson, E. P., and Maldonado-Ocampo, J. A.: A regional perspective on the diversity and conservation of tropical Andean fishes, Conserv. Biol., 25, 30-39, http://dx.doi.org/10.1111/j.1523-1739.2010.01568.x, 2011.

Asner, G. P., Anderson, C. B., Martin, R. E., Knapp, D. E., Tupayachi, R., Sinca, F., and Malhi, Y.: Landscape-scale changes in forest structure and functional traits along an Andes-to-Amazon elevation gradient, Biogeosciences, 11, 843-856, http://dx.doi.org/10.5194/bg-11-843-2014, 2014.

Ataroff, M., and Rada, F.: Deforestation impact on water dynamics in a Venezuelan Andean cloud forest, Ambio., 29, 440-444, http://dx.doi.org/10.1579/0044-7447-29.7.440, 2000.

Barnett, T. P., Adam, J. C., and Lettenmaier, D. P.: Potential impacts of a warming climate on water availability in snow-dominated regions, Nature, 438, 303-309, http://dx.doi.org/10.1038/nature04141, 2005.

Beighley, R. E., Eggert, K. G., Dunne, T., He, Y., Gummadi, V., and Verdin, K. L.: Simulating hydrologic and hydraulic processes throughout the Amazon River Basin, Hydrol. Process., 23, 1221-1235, http://dx.doi.org/10.1002/hyp.7252, 2009.

Bendix, J., Rollenbeck, R., Richter, M., Fabian, P., and Emck, P.: Climate Gradients in a Tropical Mountain Ecosystem of Ecuador, in: Gradients in a tropical mountain ecosystem of Ecuador, edited by: Beck, E., Bendix, J., Kottke, I., Makeschin, F., and Mosandl, R., Ecological Studies, Springer Berlin Heidelberg, 63-73, 2008.

Bookhagen, B., and Strecker, M. R.: Orographic barriers, high-resolution TRMM rainfall, and relief variations along the eastern Andes, Geophys. Res. Lett., 35, L06403, http://dx.doi.org/10.1029/2007GL032011, 2008.

Bouchez, J., Gaillardet, J., Lupker, M., Louvat, P., France-Lanord, C., Maurice, L., Armijos, E., and Moquet, J.-S.: Floodplains of large rivers: Weathering reactors or simple silos?, Chem. Geol., 332–333, 166-184, http://dx.doi.org/10.1016/j.chemgeo.2012.09.032, 2012.

Brodersen, C., Pohl, S., Lindenlaub, M., Leibundgut, C., and Wilpert, K. v.: Influence of vegetation structure on isotope content of throughfall and soil water, Hydrol. Process., 14, 1439-1448, 2000.

Bruijnzeel, L. A., and Veneklaas, E. J.: Climatic conditions and tropical montane forest productivity: The fog has not lifted yet, Ecology, 79, 3-9, http://dx.doi.org/10.1890/0012-9658(1998)079[0003:CCATMF]2.0.CO;2, 1998.

Bruijnzeel, L. A.: Hydrological functions of tropical forests: not seeing the soil for the trees?, Agr Ecosyst Environ, 104, 185-228, http://dx.doi:10.1016/j.agee.2004.01.015, 2004.
Bruijnzeel, L. A., Kappelle, M., Mulligan, M., and Scatena, F. N.: Tropical montane cloud forests: state of knowledge and sustainability perspectives in a changing world, in: Tropical Montane Cloud Forests. Science for Conservation and Management, edited by: Hamilton, L. S., Bruijnzeel, L. A., and Scatena, F. N., Cambridge University Press, Cambridge, UK, 691-740, 2010.
Bruijnzeel, L. A., Mulligan, M., and Scatena, F. N.: Hydrometeorology of tropical montane cloud forests: emerging patterns, Hydrol. Process., 25, 465-498, http://dx.doi.org/10.1002/hyp.7974, 2011.
Bubb, P., May, I., Miles, L., and Sayer, J.: Cloud forest agenda, UNEP-World Conservation Monitoring Centre, UNEP World Conservation Monitoring Centre, Cambridge, UK, 2004.
Bush, M. B., Silman, M. R., and Urrego, D. H.: 48,000 Years of Climate and Forest Change in a Biodiversity Hot Spot, Science, 303, 827-829, http://dx.doi.org/10.1126/science.1090795, 2004.
Buytaert, W., and Beven, K.: Models as multiple working hypotheses: Hydrological simulation of tropical alpine wetlands, Hydrol. Process., 25, 1784-1799, http://dx.doi.org/10.1002/hyp.7936, 2011.
Caballero, L. A., Easton, Z. M., Richards, B. K., and Steenhuis, T. S.: Evaluating the bio-hydrological impact of a cloud forest in Central America using a semi-distributed water balance model, J Hydrol Hydromech, 61, 9-20b, http://doi.dx.org/10.2478/jhh-2013-0003, 2013.
Calmels, D., Galy, A., Hovius, N., Bickle, M., West, A. J., Chen, M. C., and Chapman, H.: Contribution of deep groundwater to the weathering budget in a rapidly eroding mountain belt, Taiwan, Earth Planet. Sc. Lett., 303, 48-58, http://dx.doi.org/10.1016/j.epsl.2010.12.032, 2011.
Cappa, C. D., Hendricks, M. B., DePaolo, D. J., and Cohen, R. C.: Isotopic fractionation of water during evaporation, J. Geophys. Res.-Atmos., 108, 4525, http://dx.doi.org/10.1029/2003JD003597, 2003.
Carlotto Caillaux, V. S., Rodriguez, G., Fernando, W., Roque, C., Dionicio, J., and Chávez, R.: Geología de los cuadrángulos de Urubamba y Calca, Instituto Geológica Nacional, Lima, Peru, 1996.
Célleri, R., and Feyen, J.: The hydrology of tropical Andean ecosystems: importance, knowledge status, and perspectives, Mt. Res. Dev., 29, 350-355, http://dx.doi.org/10.1659/mrd.00007, 2009.
Chen, Y.-C., and Chiu, C.-L.: A fast method of flood discharge estimation, Hydrol. Process., 18, 1671-1684, http://dx.doi.org/10.1002/hyp.1476, 2004.
Clark, K. E., Hilton, R. G., West, A. J., Malhi, Y., Gröcke, D. R., Bryant, C. L., Ascough, P. L., Robles Caceres, A., and New, M.: New views on “old” carbon in the Amazon River: Insight from the source of organic carbon eroded from the Peruvian Andes, Geochem. Geophy. Geosy., 14, 1644-1659, http://dx.doi.org/10.1002/ggge.20122, 2013.
Consbio: Ecosistemas Terrestres de Peru (Data Basin Dataset) for ArcGIS, The Nature Conservancy/NatureServe Covallis, Oragon, USA, (last access: April 2012), 2011.
Craig, H.: Standard for Reporting Concentrations of Deuterium and Oxygen-18 in Natural Waters, Science, 133, 1833-1834, http://dx.doi.org/10.1126/science.133.3467.1833, 1961.
Crespo, P. J., Feyen, J., Buytaert, W., Bücker, A., Breuer, L., Frede, H. G., and Ramírez, M.: Identifying controls of the rainfall–runoff response of small catchments in the tropical Andes (Ecuador), J. Hydrol., 407, 164-174, http://dx.doi.org/10.1016/j.jhydrol.2011.07.021, 2011.
Crespo, P. J., Feyen, J., Buytaert, W., Célleri, R., Frede, H.-G., Ramírez, M., and Breuer, L.: Development of a conceptual model of the hydrologic response of tropical Andean micro-catchments in Southern Ecuador, Hydrol. Earth Syst. Sc., 9, 2475-2510, http://dx.doi.org/10.5194/hessd-9-2475-2012, 2012.
Dansgaard, W.: Stable isotopes in precipitation, Tellus, 16, 436-468, http://dx.doi.org/10.1111/j.2153-3490.1964.tb00181.x, 1964.

761 Dawson, T. E.: Fog in the California redwood forest: ecosystem inputs and use by plants, Oecologia,
762 117, 476-485, http://dx.doi.org/10.1007/s004420050683, 1998.
763 Dawson, T. E., and Ehleringer, J. R.: Plants, isotopes and water use: a catchment-scale perspective,
764 in: Isotope tracers in catchment hydrology, edited by: Kendall, C., and McDonnell, J. J.,
765 Elsevier, Amsterdam, 165-202, 1998.
766 Domenico, P. A., and Schwartz, F. W.: Physical and chemical hydrogeology, 2 ed., John Wiley & Sons,
767 New York, 1998.
768 Dunne, T., Mertes, L. A. K., Meade, R. H., Richey, J. E., and Forsberg, B. R.: Exchanges of sediment
769 between the flood plain and channel of the Amazon River in Brazil, Geol. Soc. Am. Bull., 110,
770 450-467, http://dx.doi.org/10.1130/0016-7606(1998)110<0450:eosbtf>2.3.co;2, 1998.
771 Eugster, W., Burkard, R., Holwerda, F., Scatena, F. N., and Bruijnzeel, L. A.: Characteristics of fog and
772 fogwater fluxes in a Puerto Rican elfin cloud forest, Agr. Forest Meteorol., 139, 288-306,
773 http://dx.doi.org/10.1016/j.agrformet.2006.07.008, 2006.
774 Farr, T. G., Rosen, P. A., Caro, E., Crippen, R., Duren, R., Hensley, S., Kobrick, M., Paller, M.,
775 Rodriguez, E., Roth, L., Seal, D., Shaffer, S., Shimada, J., Umland, J., Werner, M., Oskin, M.,
776 Burbank, D., and Alsdorf, D.: The Shuttle Radar Topography Mission, Rev. Geophys., 45,
777 RG2004, http://dx.doi.org/10.1029/2005RG000183, 2007.
778 Feeley, K. J., Silman, M. R., Bush, M. B., Farfan, W., Cabrera, K. G., Malhi, Y., Meir, P., Revilla, N. S.,
779 Quisiyupanqui, M. N. R., and Saatchi, S.: Upslope migration of Andean trees, J. Biogeogr., 38,
780 783-791, http://dx.doi.org/10.1111/j.1365-2699.2010.02444.x, 2011.
781 Fisher, J. B., Tu, K. P., and Baldocchi, D. D.: Global estimates of the land–atmosphere water flux
782 based on monthly AVHRR and ISLSCP-II data, validated at 16 FLUXNET sites, Remote Sens.
783 Environ., 112, 901-919, http://dx.doi.org/10.1016/j.rse.2007.06.025, 2008.
784 Fisher, J. B., Malhi, Y., Bonal, D., Da Rocha, H. R., De Araujo, A. C., Gamo, M., Goulden, M. L., Hirano,
785 T., Huete, A. R., and Kondo, H.: The land–atmosphere water flux in the tropics, Glob. Change
786 Biol., 15, 2694-2714, http://dx.doi.org/10.1111/j.1365-2486.2008.01813.x, 2009.
787 Froehlich, K., Gibson, J. J., and Aggarwal, P.: Deuterium excess in precipitation and its climatological
788 significance, Proceeding of Study of Environmental Change Using Isotope Techniques,
789 Vienna, Austria, 23-27 April 2001, IAEA-CSP-13/P, 54-66, 2002.
790 Frumau, K. F. A., Bruijnzeel, L. A., and Tobón, C.: Precipitation measurement and derivation of
791 precipitation inclination in a windy mountainous area in northern Costa Rica, Hydrol.
792 Process., 25, 499-509, http://dx.doi.org/10.1002/hyp.7860, 2011.
793 Gaillardet, J., Dupré, B., Louvat, P., and Allègre, C. J.: Global silicate weathering and CO_2 consumption
794 rates deduced from the chemistry of large rivers, Chem. Geol., 159, 3-30,
795 http://dx.doi.org/10.1016/S0009-2541(99)00031-5, 1999.
796 García-Santos, G., and Bruijnzeel, L. A.: Rainfall, fog and throughfall dynamics in a subtropical ridge
797 top cloud forest, National Park of Garajonay (La Gomera, Canary Islands, Spain), Hydrol.
798 Process., 25, 411-417, http://dx.doi.org/10.1002/hyp.7760, 2011.
799 Gascoyne, M., and Kamineni, D.: The hydrogeochemistry of fractured plutonic rocks in the Canadian
800 Shield, Applied Hydrogeology, 2, 43-49, 1994.
801 Gat, J. R.: Oxygen and hydrogen isotopes in the hydrologic cycle, Annu. Rev. Earth Pl. Sc., 24, 225-
802 262, 1996.
803 Giambelluca, T. W., and Gerold, G.: Hydrology and biogeochemistry of tropical montane cloud
804 forests, in: Forest Hydrology and Biogeochemistry, edited by: Levia, F. L., Carlyle-Moses, D.,
805 and Tanaka, T., Springer, Netherlands, 221-259, 2011.
806 Gibbon, A., Silman, M. R., Malhi, Y., Fisher, J. B., Meir, P., Zimmermann, M., Dargie, G. C., Farfan, W.
807 R., and Garcia, K. C.: Ecosystem carbon storage across the grassland-forest transition in the
808 high Andes of Manu National Park, Peru, Ecosystems, 13, 1097-1111,
809 http://dx.doi.org/10.1007/s10021-010-9376-8, 2010.
810 Gibbs, R. J.: Amazon River - Environmental factors that control its dissolved and suspended load,
811 Science, 156, 1734-1737, http://dx.doi.org/10.1126/science.156.3783.1734, 1967.

812 Girardin, C. A. J., Malhi, Y., Aragao, L. E. O. C., Mamani, M., Huasco, W. H., Durand, L., Feeley, K. J.,
813 Rapp, J., Silva-Espejo, J. E., Silman, M., Salinas, N., and Whittaker, R. J.: Net primary
814 productivity allocation and cycling of carbon along a tropical forest elevational transect in
815 the Peruvian Andes, Glob. Change Biol., 16, 3176-3192, http://dx.doi.org/10.1111/j.1365-
816 2486.2010.02235.x, 2010.
817 Girardin, C. A. J., Silva-Espejo, J. E., Doughty, C. E., Huaraca Huasco, W., Metcalfe, D. B., Durand-Baca,
818 L., Marthews, T. R., Aragao, L. E. O. C., Farfan Rios, W., García Cabrera, K., Halladay, K.,
819 Fisher, J. B., Galiano-Cabrera, D. F., Huaraca-Quispe, L. P., Alzamora-Taype, I., Equiluz-Mora,
820 L., Salinas-Revilla, N., Silman, M., Meir, P., and Malhi, Y.: Productivity and carbon allocation
821 in a tropical montane cloud forest of the Peruvian Andes, Plant Ecology and Diversity, 7, 107-
822 123, http://dx.doi.org/10.1080/17550874.2013.820222, 2014.
823 Goldsmith, G. R., Muñoz-Villers, L. E., Holwerda, F., McDonnell, J. J., Asbjornsen, H., and Dawson, T.
824 E.: Stable isotopes reveal linkages among ecohydrological processes in a seasonally dry
825 tropical montane cloud forest, Ecohydrology, 5, 779-790, http://dx.doi.org/10.1002/eco.268,
826 2012.
827 Goller, R., Wilcke, W., Leng, M. J., Tobschall, H. J., Wagner, K., Valarezo, C., and Zech, W.: Tracing
828 water paths through small catchments under a tropical montane rain forest in south Ecuador
829 by an oxygen isotope approach, J. Hydrol., 308, 67-80,
830 http://dx.doi.org/10.1016/j.jhydrol.2004.10.022, 2005.
831 Gomez-Peralta, D., Oberbauer, S. F., McClain, M. E., and Philippi, T. E.: Rainfall and cloud-water
832 interception in tropical montane forests in the eastern Andes of Central Peru, Forest Ecol
833 Manag, 255, 1315-1325, http://dx.doi.org/10.1016/j.foreco.2007.10.058, 2008.
834 Gustard, A., Bullock, A., and Dixon, J.: Low flow estimation in the United Kingdom, Low flow
835 estimation in the United Kingdom, Institute of Hydrology, Wallingford, UKpp., 1992.
836 Guswa, A. J., Rhodes, A. L., and Newell, S. E.: Importance of orographic precipitation to the water
837 resources of Monteverde, Costa Rica, Adv Water Resour, 30, 2098-2112,
838 http://dx.doi.org/10.1016/j.advwatres.2006.07.008, 2007.
839 Guyot, J. L., Fillzola, N., Quintanilla, J., and Cortez, J.: Dissolved solids and suspended sediment yields
840 in the Rio Madeira basin, from the Bolivian Andes to the Amazon, IAHS-AISH P., 236, 55-64,
841 1996.
842 Halladay, K.: Cloud characteristics of the Andes/Amazon transition zone, DPhil, School of Geography
843 and the Environment, University of Oxford, Oxford, UK, 260 pp., 2011.
844 Halladay, K., Malhi, Y., and New, M.: Cloud frequency climatology at the Andes/Amazon transition: 1.
845 Seasonal and diurnal cycles, J. Geophys. Res., 117, D23102,
846 http://dx.doi.org/10.1029/2012JD017770, 2012a.
847 Halladay, K., Malhi, Y., and New, M.: Cloud frequency climatology at the Andes/Amazon transition: 2.
848 Trends and variability, J. Geophys. Res., 117, D23103,
849 http://dx.doi.org/10.1029/2012JD017789, 2012b.
850 Hillyer, R., and Silman, M. R.: Changes in species interactions across a 2.5 km elevation gradient:
851 effects on plant migration in response to climate change, Glob. Change Biol., 16, 3205-3214,
852 http://dx.doi.org/10.1111/j.1365-2486.2010.02268.x, 2010.
853 Holwerda, F., Burkard, R., Eugster, W., Scatena, F., Meesters, A., and Bruijnzeel, L.: Estimating fog
854 deposition at a Puerto Rican elfin cloud forest site: comparison of the water budget and
855 eddy covariance methods, Hydrol Process, 20, 2669-2692,
856 http://dx.doi.org/10.1002/hyp.6065, 2006.
857 Holwerda, F., Bruijnzeel, L. A., Muñoz-Villers, L. E., Equihua, M., and Asbjornsen, H.: Rainfall and
858 cloud water interception in mature and secondary lower montane cloud forests of central
859 Veracruz, Mexico, J. Hydrol., 384, 84-96, http://dx.doi.org/10.1016/j.jhydrol.2010.01.012,
860 2010a.
861 Holwerda, F., Bruijnzeel, L. A., Oord, A. L., and Scatena, F. N.: Fog interception in a Puerto Rican elfin
862 cloud forest: a Wet-canopy Water budget approach, in: Tropical Montane Cloud Forests:

Science for Conservation and Management, edited by: Bruijnzeel, L. A., Scatena, F. N., and Hamilton, L. S., Cambridge University Press, Cambridge, UK, 282-292, 2010b.
Huaraca Huasco, W., Girardin, C. A. J., Doughty, C. E., Metcalfe, D. B., Baca, L. D., Silva-Espejo, J. E., Cabrera, D. G., Aragão, L. E. O., Davila, A. R., Marthews, T. R., Huaraca-Quispe, L. P., Alzamora-Taype, I., Eguiluz-Mora, L., Farfan-Rios, W., Cabrera, K. G., Halladay, K., Salinas-Revilla, N., Silman, M., Meir, P., and Malhi, Y.: Seasonal production, allocation and cycling of carbon in two mid-elevation tropical montane forest plots in the Peruvian Andes, Plant Ecology and Diversity, 1-2, 125-142, http://dx.doi.org/10.1080/17550874.2013.819042, 2014.
INGEMMET: GEOCATMIN - Geologia integrada por proyectos regionales, Instituto Geológico Minero Metalúrgico Lima, Peru, (last access: March 2013), 2013.
Jardine, P. M., Sanford, W. E., Gwo, J. P., Reedy, O. C., Hicks, D. S., Riggs, J. S., and Bailey, W. B.: Quantifying diffusive mass transfer in fractured shale bedrock, Water Resour. Res., 35, 2015-2030, 1999.
Killeen, T. J., Douglas, M., Consiglio, T., Jørgensen, P. M., and Mejia, J.: Dry spots and wet spots in the Andean hotspot, J. Biogeogr., 34, 1357-1373, http://dx.doi.org/10.1111/j.1365-2699.2006.01682.x, 2007.
Kim, H., Bishop, J. K. B., Dietrich, W. E., and Fung, I. Y.: Process dominance shift in solute chemistry as revealed by long-term high-frequency water chemistry observations of groundwater flowing through weathered argillite underlying a steep forested hillslope, Geochim Cosmochim Ac, 140, 1-19, http://dx.doi.org/10.1016/j.gca.2014.05.011, 2014.
Kuntz, B. W., Rubin, S., Berkowitz, B., and Singha, K.: Quantifying solute transport at the Shale Hills Critical Zone Observatory, Vadose Zone J, 10, 843-857, http://dx.doi.org/10.2136/vzj2010.0130, 2011.
Lambs, L., Horwath, A., Otto, T., Julien, F., and Antoine, P. O.: Isotopic values of the Amazon headwaters in Peru: comparison of the wet upper Río Madre de Dios watershed with the dry Urubamba-Apurimac river system, Rapid Commun. Mass Sp., 26, 775-784, http://dx.doi.org/10.1002/rcm.6157, 2012.
Larsen, M. C.: Analysis of 20th century rainfall and streamflow to characterize drought and water resources in Puerto Rico, Phys Geogr, 21, 494-521, http://dx.doi:10.1080/02723646.2000.10642723, 2000.
Lehner, B., Verdin, K., and Jarvis, A.: New Global Hydrography Derived From Spaceborne Elevation Data, Eos Trans. AGU, 89, 93-94, http://dx.doi.org/10.1029/2008EO100001, 2008.
Letts, M. G., and Mulligan, M.: The impact of light quality and leaf wetness on photosynthesis in north-west Andean tropical montane cloud forest, J. Trop. Ecol., 21, 549-557, http://dx.doi.org/10.1017/S0266467405002488, 2005.
Lowman, L. E. L., and Barros, A. P.: Investigating Links between Climate and Orography in the central Andes: Coupling Erosion and Precipitation using a Physical-statistical Model, J Geophys Res-Earth, http://dx.doi.org/10.1002/2013JF002940, 2014.
Malhi, Y., Silman, M., Salinas, N., Bush, M., Meir, P., and Saatchi, S.: Introduction: Elevation gradients in the tropics: laboratories for ecosystem ecology and global change research, Glob. Change Biol., 16, 3171-3175, http://dx.doi.org/10.1111/j.1365-2486.2010.02323.x, 2010.
Marengo, J. A., Soares, W. R., Saulo, C., and Nicolini, M.: Climatology of the low-level jet east of the Andes as derived from the NCEP-NCAR reanalyses: Characteristics and temporal variability, J. Climate, 17, 2261-2280, 2004.
Marzol-Jaén, M. V., Sanchez-Megía, J., and García-Santos, G.: Effects of fog on climatic conditions at a sub-tropical montane cloud forest site in northern Tenerife (Canary Islands, Spain), in: Tropical Montane Cloud Forests: Science for Conservation and Management, edited by: Bruijnzeel, L. A., Scatena, F. N., and Hamilton, L. S., Cambridge University Press, Cambridge, UK, 359-364, 2010.

McClain, M. E., and Naiman, R. J.: Andean influences on the biogeochemistry and ecology of the Amazon River, Bioscience, 58, 325-338, http://dx.doi.org/10.1641/b580408, 2008.
McJannet, D., Wallace, J., and Reddell, P.: Precipitation interception in Australian tropical rainforests: II. Altitudinal gradients of cloud interception, stemflow, throughfall and interception, Hydrol. Process., 21, 1703-1718, http://dx.doi.org/10.1002/hyp.6346, 2007.
McJannet, D. L., Wallace, J. S., and Reddell, P.: Comparative water budgets of a lower and an upper montane cloud forest in the Wet Tropics of northern Australia, in: Tropical Montane Cloud Forests. Science for Conservation and Management, edited by: Bruijnzeel, L. A., and Scatena, F. N., Cambrige University Press, Cambridge, UK, 479-490, 2010.
Meade, R. H., Dunne, T., Richey, J. E., Santos, U. D., and Salati, E.: Storage and remobilisation of suspended sediment in the lower Amazon River of Brazil, Science, 228, 488-490, http://dx.doi.org/10.1126/science.228.4698.488, 1985.
Milliman, J. D., and Farnsworth, K. L.: Runoff, erosion, and delivery to the coastal ocean, in: River discharge to the coastal ocean: a global synthesis, Cambridge University Press, Cambridge, UK, 13-69, 2011.
Morris, D. A., and Johnson, A. I.: Summary of Hydrologic and Physical Properties of Rock and Soil Materials, as Analyzed by the Hydrologic Laboratory of the US Geological Survey 1948-60, Summary of Hydrologic and Physical Properties of Rock and Soil Materials, as Analyzed by the Hydrologic Laboratory of the US Geological Survey 1948-60, US Government Printing Office, Washington, USA, 46 pp., 1967.
Mulligan, M., and Burke, S. M.: FIESTA: Fog Interception for the Enhancement of Streamflow in Tropical Areas, FIESTA: Fog Interception for the Enhancement of Streamflow in Tropical Areas, for KCL/AMBIOTEK Contribution to DFID-FRP project R7991pp., 2005.
Mulligan, M.: Modelling the tropics-wide extent and distribution of cloud forest and cloud forest loss, with implications for conservation priority, in: Tropical Montane Cloud Forests. Science for Conservation and Management, edited by: Bruijnzeel, L. A., Scatena, F. N., and Hamilton, L. S., Cambridge University Press, Cambridge, UK, 14-38, 2010.
Muñoz-Villers, L. E., Holwerda, F., Gómez-Cárdenas, M., Equihua, M., Asbjornsen, H., Bruijnzeel, L. A., Marín-Castro, B. E., and Tobón, C.: Water balances of old-growth and regenerating montane cloud forests in central Veracruz, Mexico, J. Hydrol., 462, 53-66, http://dx.doi.org/10.1016/j.jhydrol.2011.01.062, 2012.
Muñoz-Villers, L. E., and McDonnell, J. J.: Runoff generation in a steep, tropical montane cloud forest catchment on permeable volcanic substrate, Water Resour. Res., 48, W09528, http://dx.doi.org/10.1029/2011WR011316, 2012.
Myers, N., Mittermeier, R. A., Mittermeier, C. G., Da Fonseca, G. A. B., and Kent, J.: Biodiversity hotspots for conservation priorities, Nature, 403, 853-858, http://dx.doi.org/10.1038/35002501, 2000.
Ortega, H., and Hidalgo, M.: Freshwater fishes and aquatic habitats in Peru: Current knowledge and conservation, Aquat. Ecosyst. Health, 11, 257-271, http://dx.doi.org/10.1080/14634980802319135, 2008.
Phillips, D. L., and Gregg, J. W.: Uncertainty in source partitioning using stable isotopes, Oecologia, 127, 171-179, http://dx.doi.org/10.1007/s004420000578, 2001.
Postel, S. L., and Thompson, B. H.: Watershed protection: Capturing the benefits of nature's water supply services, Natural Resources Forum, 29, 98-108, http://dx.doi.org/10.1111/j.1477-8947.2005.00119.x, 2005.
Priestley, C. H. B., and Taylor, R. J.: On the Assessment of Surface Heat Flux and Evaporation Using Large-Scale Parameters, Mon. Weather Rev., 100, 81-92, http://dx.doi.org/10.1175/1520-0493(1972)100<0081:otaosh>2.3.co;2, 1972.
Rapp, J. M., and Silman, M. R.: Diurnal, seasonal, and altitudinal trends in microclimate across a tropical montane cloud forest, Clim. Res., 55, 17-32, http://dx.doi.org/10.3354/cr01127, 2012.

964 Rapp, J. M., and Silman, M. R.: Epiphyte response to drought and experimental warming in an
965 Andean cloud forest [v2; ref status: indexed, http://f1000r.es/3le], F1000Res., 3,
966 http://dx.doi.org/10.12688/f1000research.3-7.v2, 2014.
967 Rhodes, A. L., Guswa, A. J., and Newell, S. E.: Seasonal variation in the stable isotopic composition of
968 precipitation in the tropical montane forests of Monteverde, Costa Rica, Water Resour. Res.,
969 42, W11402, http://dx.doi.org/10.1029/2005WR004535, 2006.
970 Richey, J. E., Meade, R. H., Salati, E., Devol, A. H., Nordin, C. F., and Dossantos, U.: Water discharge
971 and suspended sediment concentrations in the Amazon River 1982-1984, Water Resour.
972 Res., 22, 756-764, http://dx.doi.org/10.1029/WR022i005p00756, 1986.
973 Richey, J. E., Valarezo, C., Valarezo, C., and Valarezo, C.: Biogeochemistry of carbon in the Amazon
974 River, Limnol. Oceanogr., 35, 352-371, 1990.
975 Rozanski, K., Araguás-Araguás, L., and Gonfiantini, R.: Isotopic Patterns in Modern Global
976 Precipitation, in: Climate Change in Continental Isotopic Records, edited by: Swart, P. K.,
977 Lohman, K. C., McKenzie, J., and Savin, S., American Geophysical Union, Washington, DC, 1-
978 36, 1993.
979 Salati, E., Dall'Olio, A., Matsui, E., and Gat, J. R.: Recycling of water in the Amazon basin: an isotopic
980 study, Water Resour. Res., 15, 1250-1258, http://dx.doi.org/10.1029/WR015i005p01250,
981 1979.
982 Salinas, N., Malhi, Y., Meir, P., Silman, M., Roman Cuesta, R., Huaman, J., Salinas, D., Huaman, V.,
983 Gibaja, A., Mamani, M., and Farfan, F.: The sensitivity of tropical leaf litter decomposition to
984 temperature: results from a large-scale leaf translocation experiment along an elevation
985 gradient in Peruvian forests, New Phytol., 189, 967-977, http://dx.doi.org/10.1111/j.1469-
986 8137.2010.03521.x, 2011.
987 Scheel, M. L. M., Rohrer, M., Huggel, C., Santos Villar, D., Silvestre, E., and Huffman, G. J.: Evaluation
988 of TRMM Multi-satellite Precipitation Analysis (TMPA) performance in the Central Andes
989 region and its dependency on spatial and temporal resolution, Hydrol. Earth Syst. Sc., 15,
990 2649-2663, http://dx.doi.org/10.5194/hess-15-2649-2011, 2011.
991 Schellekens, J.: CQ-FLOW: A distributed hydrological model for the prediction of impacts of land-
992 cover change, with spatial reference to the Rio Chiquito catchment, northwest Costa Rica,
993 CQ-FLOW: A distributed hydrological model for the prediction of impacts of land-cover
994 change, with spatial reference to the Rio Chiquito catchment, northwest Costa Rica, Vrije
995 Universiteit Amsterdam and Forestry Research Programme, Amsterdam, The Netherlands,
996 71 pp., 2006.
997 Schmid, S., Burkard, R., Frumau, K. F. A., Tobon, C., Bruijnzeel, L. A., Siegwolf, R., and Eugster, W.:
998 The wet-canopy water balance of a Costa Rican cloud forest during the dry season, in:
999 Tropical Montane Cloud Forests: Science for Conservation and Management, edited by:
1000 Bruijnzeel, L. A., Scatena, F. N., and Hamilton, L. S., Cambridge University Press, Cambridge,
1001 UK, 302-308, 2010.
1002 Scholl, M., Eugster, W., and Burkard, R.: Understanding the role of fog in forest hydrology: stable
1003 isotopes as tools for determining input and partitioning of cloud water in montane forests,
1004 Hydrol. Process., 25, 353-366, http://dx.doi.org/10.1002/hyp.7762, 2011.
1005 Scholl, M. A., Giambelluca, T. W., Gingerich, S. B., Nullet, M. A., and Loope, L. L.: Cloud water in
1006 windward and leeward mountain forests: The stable isotope signature of orographic cloud
1007 water, Water Resour. Res., 43, W12411, http://dx.doi.org/10.1029/2007WR006011, 2007.
1008 Scholl, M. A., and Murphy, S. F.: Precipitation isotopes link regional climate patterns to water supply
1009 in a tropical mountain forest, eastern Puerto Rico, Water Resour. Res., 50, 4305-4322,
1010 http://dx.doi.org/10.1002/2013WR014413, 2014.
1011 SENAMHI: Clima: Datos históricos Peru, http://www.senamhi.gob.pe/main_mapa.php?t=dHi, (last
1012 access: May 2012), 2012.
1013 Squeo, F. A., Warner, B. G., Aravena, R., and Espinoza, D.: Bofedales: high altitude peatlands of the
1014 central Andes, Rev. Chil. Hist. Nat., 79, 245-255, 2006.

1015 Stallard, R. F., and Edmond, J. M.: Geochemistry of the Amazon: 2. The influence of geology and
1016 weathering environment on the dissolved load, J. Geophys. Res.-Oceans, 88, 9671-9688,
1017 http://dx.doi.org/10.1029/JC088iC14p09671, 1983.
1018 Teh, Y. A., Diem, T., Jones, S., Huaraca Quispe, L. P., Baggs, E., Morley, N., Richards, M., Smith, P., and
1019 Meir, P.: Methane and nitrous oxide fluxes across an elevation gradient in the tropical
1020 Peruvian Andes, Biogeosciences, 11, 2325-2339, http://dx.doi.org/10.5194/bg-11-2325-
1021 2014, 2014.
1022 Thome, C. R., and Zevenbergen, L. W.: Estimating mean velocity in mountain rivers, J. Hydraul. Eng.,
1023 111, 612-624, 1985.
1024 Thorburn, P. J., Hatton, T. J., and Walker, G. R.: Combining measurements of transpiration and stable
1025 isotopes of water to determine groundwater discharge from forests, J Hydrol., 150, 563-587,
1026 http://dx.doi.org/10.1016/0022-1694(93)90126-T, 1993.
1027 Timbe, E., Windhorst, D., Crespo, P., Frede, H. G., Feyen, J., and Breuer, L.: Understanding
1028 uncertainties when inferring mean transit times of water trough tracer-based lumped-
1029 parameter models in Andean tropical montane cloud forest catchments, Hydrol. Earth Syst.
1030 Sc., 18, 1503-1523, http://dx.doi.org/10.5194/hess-18-1503-2014, 2014.
1031 Tipper, E. T., Bickle, M. J., Galy, A., West, A. J., Pomiès, C., and Chapman, H. J.: The short term
1032 climatic sensitivity of carbonate and silicate weathering fluxes: insight from seasonal
1033 variations in river chemistry, Geochim. Cosmochim. Ac., 70, 2737-2754,
1034 http://dx.doi.org/10.1016/j.gca.2006.03.005, 2006.
1035 Todd, D. K., and Mays, L. W.: Groundwater Hydrology, 3, Wiley, New York, 625 pp., 1980.
1036 Tognetti, S., Aylward, B., and Bruijnzeel, L. A.: Assessment needs to support the development of
1037 arrangements for payments for ecosystem services from tropical montane cloud forests, in:
1038 Tropical Montane Cloud Forests. Science for Conservation and Management, edited by:
1039 Bruijnzeel, L. A., Scatena, F. N., and Hamilton, L. S., Cambridge University Press, Cambridge,
1040 UK, 671-685, 2010.
1041 Torres, M. A., West, A. J., and Clark, K. E.: Geomorphic regime modulates hydrologic control of
1042 chemical weathering in the Andes-Amazon, Geochim Cosmochim Ac, in review.
1043 Tovar, C., Arnillas, C. A., Cuesta, F., and Buytaert, W.: Diverging responses of tropical Andean biomes
1044 under future climate conditions, PloS one, 8, e63634,
1045 http://dx.doi.org/10.1371/journal.pone.0063634, 2013.
1046 Townsend-Small, A., McClain, M. E., Hall, B., Noguera, J. L., Llerena, C. A., and Brandes, J. A.:
1047 Suspended sediments and organic matter in mountain headwaters of the Amazon River:
1048 Results from a 1-year time series study in the central Peruvian Andes, Geochim. Cosmochim.
1049 Ac., 72, 732-740, http://dx.doi.org/10.1016/j.gca.2007.11.020, 2008.
1050 TRMM: Tropical Rainfall Measuring Mission product 3B43 v7a, NASA,
1051 http://mirador.gsfc.nasa.gov/cgi-
1052 bin/mirador/presentNavigation.pl?tree=project&project=TRMM&dataGroup=Gridded&data
1053 set=3B43:%20Monthly%200.25%20x%200.25%20degree%20merged%20TRMM%20and%20
1054 other%20sources%20estimates&version=006, access: 2 April 2013, 2013.
1055 van de Weg, M. J., Meir, P., Grace, J., and Ramos, G. D.: Photosynthetic parameters, dark respiration
1056 and leaf traits in the canopy of a Peruvian tropical montane cloud forest, Oecologia, 168, 23-
1057 34, http://dx.doi.org/10.1007/s00442-011-2068-z, 2012.
1058 van de Weg, M. J., Meir, P., Williams, M., Girardin, C., Malhi, Y., Silva-Espejo, J., and Grace, J.: Gross
1059 primary productivity of a high elevation tropical montane cloud forest, Ecosystems, 17, 751-
1060 764, http://dx.doi.org/10.1007/s10021-014-9758-4, 2014.
1061 Wilcox, B. P., Allen, B., and Bryant, F.: Description and classification of soils of the high-elevation
1062 grasslands of central Peru, Geoderma, 42, 79-94, 1988.
1063 Windhorst, D., Waltz, T., Timbe, E., Frede, H. G., and Breuer, L.: Impact of elevation and weather
1064 patterns on the isotopic composition of precipitation in a tropical montane rainforest,
1065 Hydrol. Earth Syst. Sci., 17, 409-419, http://dx.doi.org/10.5194/hess-17-409-2013, 2013.

Wittmann, H., von Blanckenburg, F., Maurice, L., Guyot, J.-L., Filizola, N., and Kubik, P. W.: Sediment production and delivery in the Amazon River basin quantified by in situ-produced cosmogenic nuclides and recent river loads, Geol. Soc. Am. Bull., 123, 934-950, http://dx.doi.org/10.1130/b30317.1, 2011.

Zadroga, F.: The hydrological importance of a montane cloud forest area of Costa Rica, in: Tropical agricultural hydrology, edited by: Lal, R., and Russell, E. W., Wiley and Sons, New York, 59-73, 1981.

Zimmermann, M., Meir, P., Bird, M. I., Malhi, Y., and Ccahuana, A. J. Q.: Climate dependence of heterotrophic soil respiration from a soil-translocation experiment along a 3000 m tropical forest altitudinal gradient, Eur. J. Soil Sci., 60, 895-906, http://dx.doi.org/10.1111/j.1365-2389.2009.01175.x, 2009.

Tables

TABLE 1: Descriptions of the Kosñipata catchment.

Catchment	Area (km^2)	Mean slope* (°)	Mean elevation* (masl)	Elevation range* (masl)	Landcover type¤ (~ %)	Geology^ (~ %)	Gauge lat/long (S, W)	Gauge elevation (masl)
Kosñipata at San Pedro	164.4	28	2805	1360 to 4000	TMCF (92.7), puna /transition (7.3)	mudstones (80), pluton intrusions (20)	13°3'37", 71°32'40"	1360
Kosñipata at Wayqecha**	48.5	26	3195	2250 to 3905	TMCF (75), puna /transition (25)	mudstones (100)	13°9'46", 71°35'21"	2250

* Based on Shuttle Radar Topography Mission (SRTM) data with a 90 m × 90 m resolution.
^ Basin geology derived from (Carlotto Caillaux et al., 1996).
¤ Landcover types were determined using 2009 Quickbird 2 imagery.
** Results presented in supplementary information.

1085

TABLE 2: Water budget components for the Kosñipata catchment at the San Pedro (SP) gauging station, for the annual period from February 2010 to January 2011. Percentages indicate fraction of the annual total for that component.

	Number of months/ days	Q ($m^3 s^{-1}$)	Runoff mm d^{-1}, (%)	Baseflow mm d^{-1} (%)	BFI*	Rainfall^ mm d^{-1} (%)	CWI mm d^{-1} (%)	AET mm d^{-1} (%)
Wet	4/121	23.1±1.3	12.13±0.68 (52)	9.41±0.77 (52)	0.77±0.04	15.00±3.08 (58)	1.37±0.70 (52)	1.87±0.37 (33)
Wet-dry	1/30	19.6±2.6	10.29±1.37 (11)	8.75±1.35 (12)	0.85±0.02	6.95±2.58 (7)	1.16±1.39 (11)	1.86±0.37 (8)
Dry	5/153	8.1±0.9	4.31±0.46 (24)	3.58±0.48 (26)	0.83±0.04	4.32±0.73 (21)	0.50±0.32 (24)	1.81±0.36 (40)
Dry-wet	2/61	11.3±1.5	5.94±0.81 (13)	3.56±0.73 (10)	0.60±0.04	7.02±1.95 (14)	0.63±0.75 (12)	2.11±0.42 (19)
Annual	12/365	14.6±0.7	7.66±0.35 (100)	5.95±0.37 (100)	0.77±0.04	8.53±1.13 (100)	0.87±0.32 (100)	1.88±0.38 (100)

Seasonal contribution as percentage of total in parenthesis.
Uncertainties are propagated 1σ errors.
* Base flow index (BFI) is the ratio of the total volume of baseflow divided by the total volume of discharge following the method outlined in Gustard et al. (1992).
^ Catchment-wide rainfall is corrected for wind-induced loss and is reported for February 2010 to January 2011 to coincide with the study period.

1086

1087

TABLE 3: Breakdown of streamflow into its sources

	n	Fraction wet season rainfall[a]	Fraction dry season rainfall[a]	Fraction cloud water[a]	Wet season rain as a source (mm month^{-1})[b]	Dry season rain as a source (mm month^{-1})[b]	Cloud water as a source (mm month^{-1})[b]	Total stream runoff (mm month^{-1})
Feb-10	28	0.62±0.04	0.24±0.04	0.11±0.03	231±16	91±17	41±13	372±38
Mar-10	2	0.62±0.15	0.25±0.16	0.10±0.12	261±70	105±72	44±56	420±41
Apr-10	2	0.65±0.14	0.21±0.14	0.11±0.12	200±49	66±49	35±42	309±41
May-10	3	0.61±0.12	0.25±0.13	0.11±0.10	143±34	59±35	27±28	235±40
Jun-10	1	0.63±0.20	0.22±0.20	0.12±0.17	103±40	36±40	19±35	163±35
Jul-10	2	0.58±0.13	0.28±0.14	0.12±0.11	61±17	28±18	13±14	105±30
Aug-10	3	0.58±0.13	0.27±0.14	0.12±0.10	51±15	24±16	10±12	87±26
Sep-10	3	0.59±0.13	0.26±0.23	0.12±0.11	42±12	19±13	8±10	70±23
Oct-10	1	0.64±0.22	0.26±0.23	0.08±0.16	127±53	51±55	16±39	199±36
Nov-10	3	0.52±0.14	0.30±0.15	0.14±0.12	86±28	50±31	23±25	164±34
Dec-10	4	0.56±0.12	0.30±0.13	0.10±0.09	188±44	98±50	35±33	333±42
Jan-11	2	0.55±0.16	0.29±0.18	0.14±0.14	186±62	99±69	46±54	339±43
Fractional contributions by season[c]								
Wet		0.59±0.07	0.27±0.08	0.11±0.05				
Wet-dry		0.65±0.14	0.21±0.14	0.11±0.12				
Dry		0.61±09	0.25±0.09	0.12±0.07				
Dry-wet		0.59±0.16	0.28±0.17	0.11±0.13				
Annual		0.60±0.05	0.26±0.05	0.11±0.04				

[a] Calculated from monthly average values of mixing model results. Reported errors are propagated uncertainty (1σ) from individual samples per month, accounting for uncertainties from the Monte Carlo mixing model (Table S7 in the Supplement).
[b] Calculated from monthly fractional contributions and monthly runoff. Reported errors are propagated uncertainty (1σ) from the mixing modelling and from the variation in stream runoff.
[c] Calculated based on runoff totals for each month, from each source, summed for a given season. Reported errors are propagated uncertainty from monthly runoff estimates from each source.
n = number of samples.

1088

1089

Figures

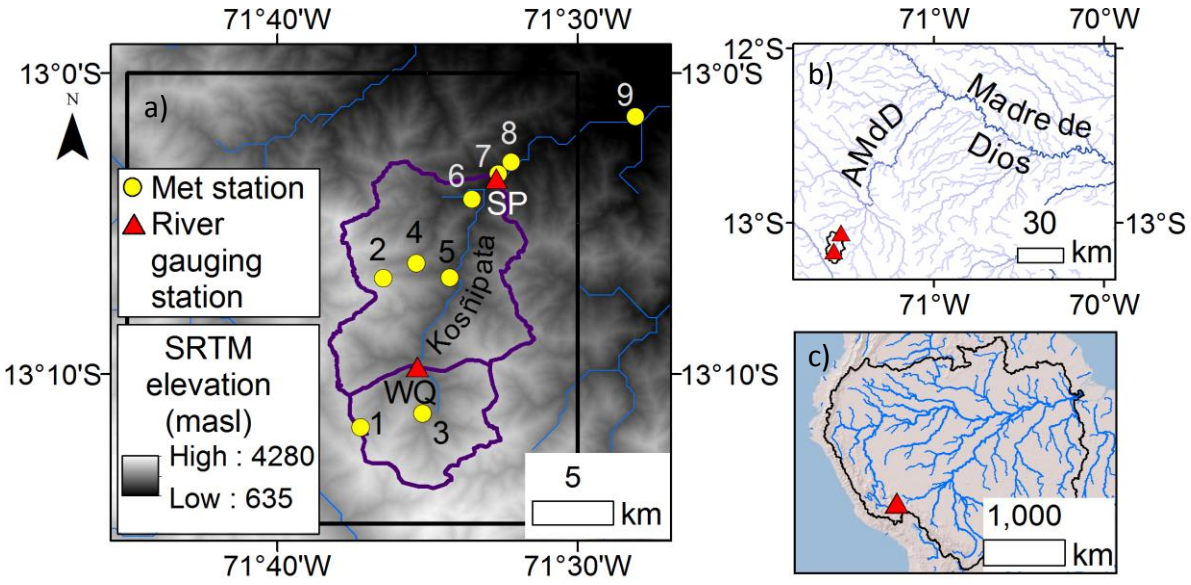

Figure 1: a) The Kosñipata catchment, Eastern Andes of Peru, showing the Kosñipata River catchment measured at the San Pedro (SP) river gauging station and the nested sub-catchment at the Wayqecha (WQ) river gauging station, overlaid on 90 m × 90 m digital elevation model (Shuttle Radar Topography Mission) (Farr et al., 2007). Black box indicates the extent of the TRMM 3B43 tile used in this study (cf. Fig. 2a). The meteorological stations used for rainfall data are numbered 1 to 9 (Table S2). b) The Kosñipata River flows into the Alto Madre de Dios (AMdD) and then into the Madre de Dios River, a major tributary of the Amazon River (c). The river network was produced from HydroSHEDS (hydrological data and maps based on shuttle elevation derivatives at multiple scales) (Lehner et al., 2008).

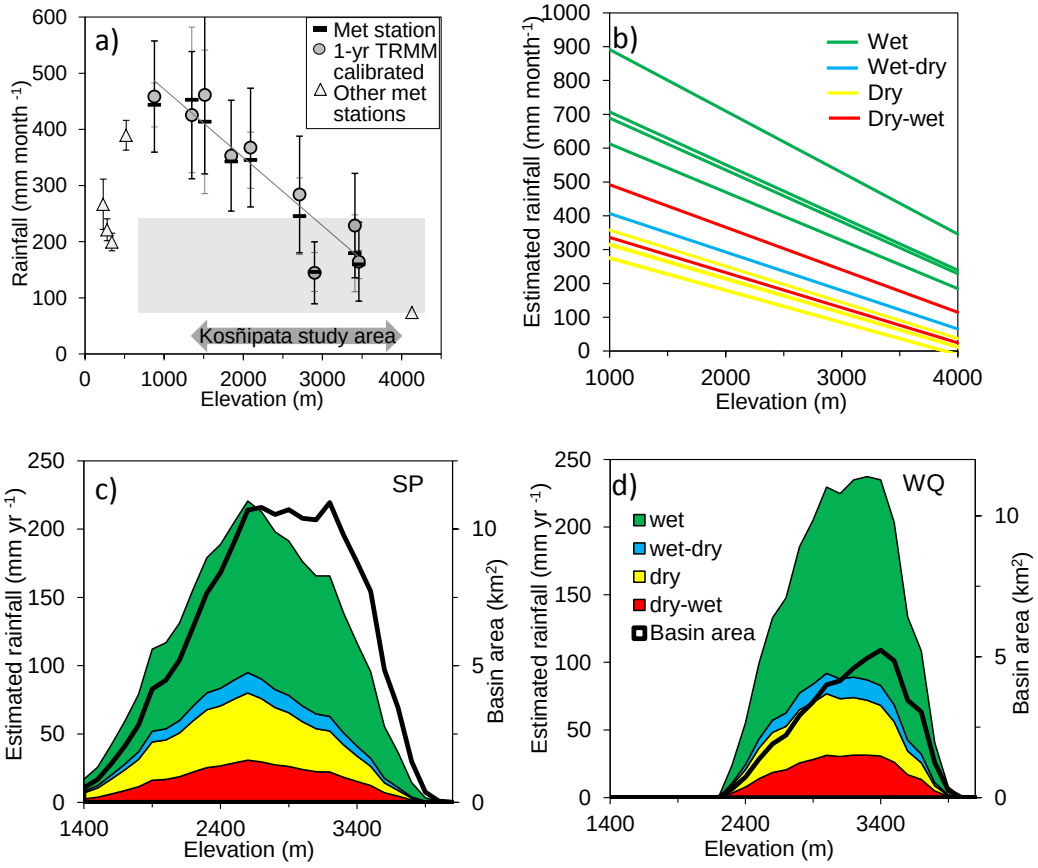

Figure 2: Mean monthly rainfall data for the 9 meteorological stations in the Kosñipata catchment study area (from ~900 to ~3500 masl) (dark dashes and light error bars) and estimated mean monthly rainfall (grey circles and dark error bars) covering the months of the 1-year study period (February 2010 to January 2011) determined using the linear regression equations for each meteorological station derived from tropical rainfall measuring mission (TRMM) data (Table S8). The grey line is the linear fit with elevation for the estimated mean monthly rainfall (mm month^{-1} = –0.1216±0.0187 × elevation + 593.16±44.94, R^2 = 0.86; P = 0.0003). The error bars are 2 × standard error of monthly data. Mean monthly rainfall for 5 meteorological stations outside of the study area but within the larger Madre de Dios Basin are also shown as triangles (Rapp and Silman, 2012). The shaded box shows the TRMM 3B43 v7a monthly mean rainfall for the 1-year study period with 2 × standard error. Elevation range is shown for the 34.5 km × 34.5 km TRMM tile. The altitudinal range of the study area is represented by the dashed lines at 1350 and 4000 masl. b) Linear regressions of estimated catchment wide rainfall by month from February 2010 to January 2011, colour-coded by season. The distribution of annual rainfall with elevation by season for the Kosñipata River is shown for the San Pedro (SP) gauging station (c) and the Wayqecha (WQ) gauging station (d) at 100 m intervals using the monthly linear regressions (b) incorporating the correction for wind-induced rainfall loss (Table S3).

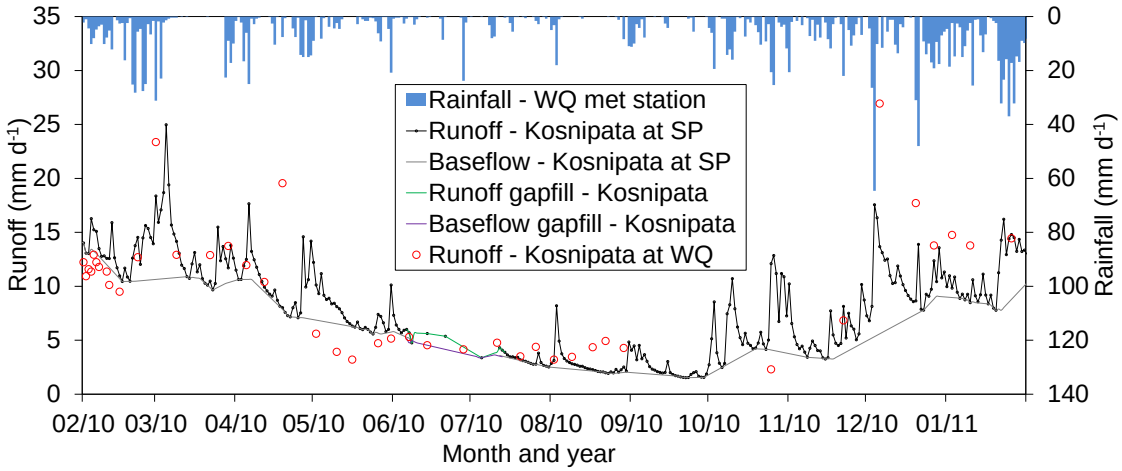

1124

1125 Figure 3: Runoff for the Kosñipata River at the San Pedro (SP) and Wayqecha (WQ) gauging
1126 stations. Rainfall (top axis) from the Wayqecha meteorological station is on the secondary
1127 axis. The Kosñipata River runoff at San Pedro and baseflow were measured nearly
1128 continuously through the year, with a 31-day gap partly in July and August that is covered by
1129 three manual measurements and the gap filled using linear interpolation. The Kosñipata River
1130 runoff at Wayqecha was measured throughout the year from a daily to a monthly interval and
1131 is discussed in the supplementary section.

1132

1133

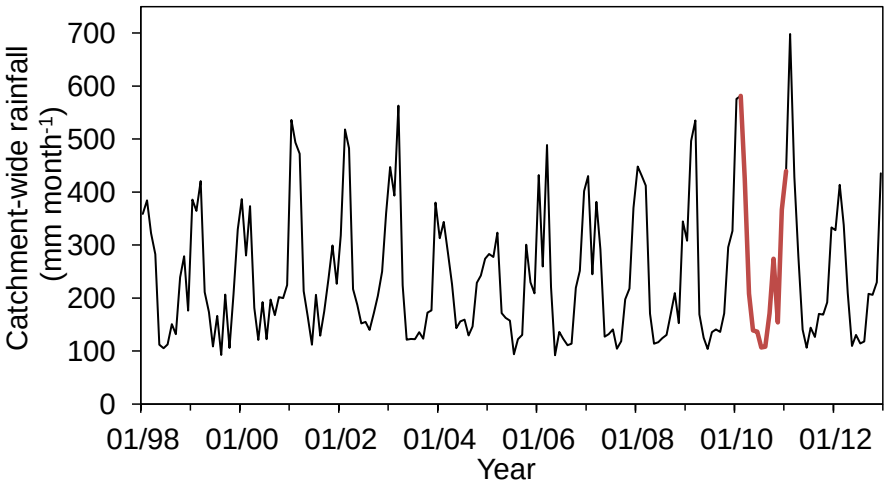

1134

1135

1136 Figure 4: Catchment wide TRMM calibrated rainfall for the Kosñipata catchment from 1998
1137 to 2012. The thick red line represents the 1-year study period.

1138

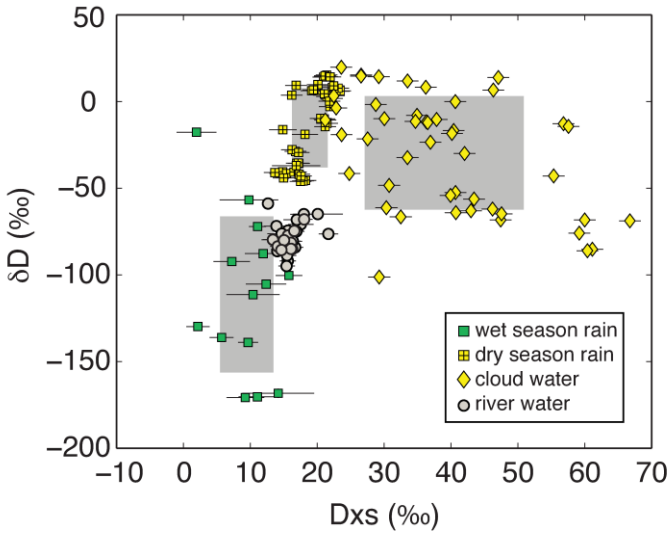

Figure 5: Hydrogen isotope ratio **(**δD, ‰) and deuterium excess (Dxs, ‰) of dry season cloud water vapour (yellow diamonds), and river water (grey circles) from the Kosñipata catchment. Rainwater samples (squares) are from the dry season (May to August, yellow) and from the wet season (December to March, green). All error bars correspond to two standard deviations. The grey shaded regions encompass the mean δD and Dxs values and one standard deviation for each end-member (i.e. wet season rainfall, dry season rainfall, and dry season cloud water vapour). The ranges defined by these grey boxes were used to generate random sets of end-member compositions for the three end-member mixing model.

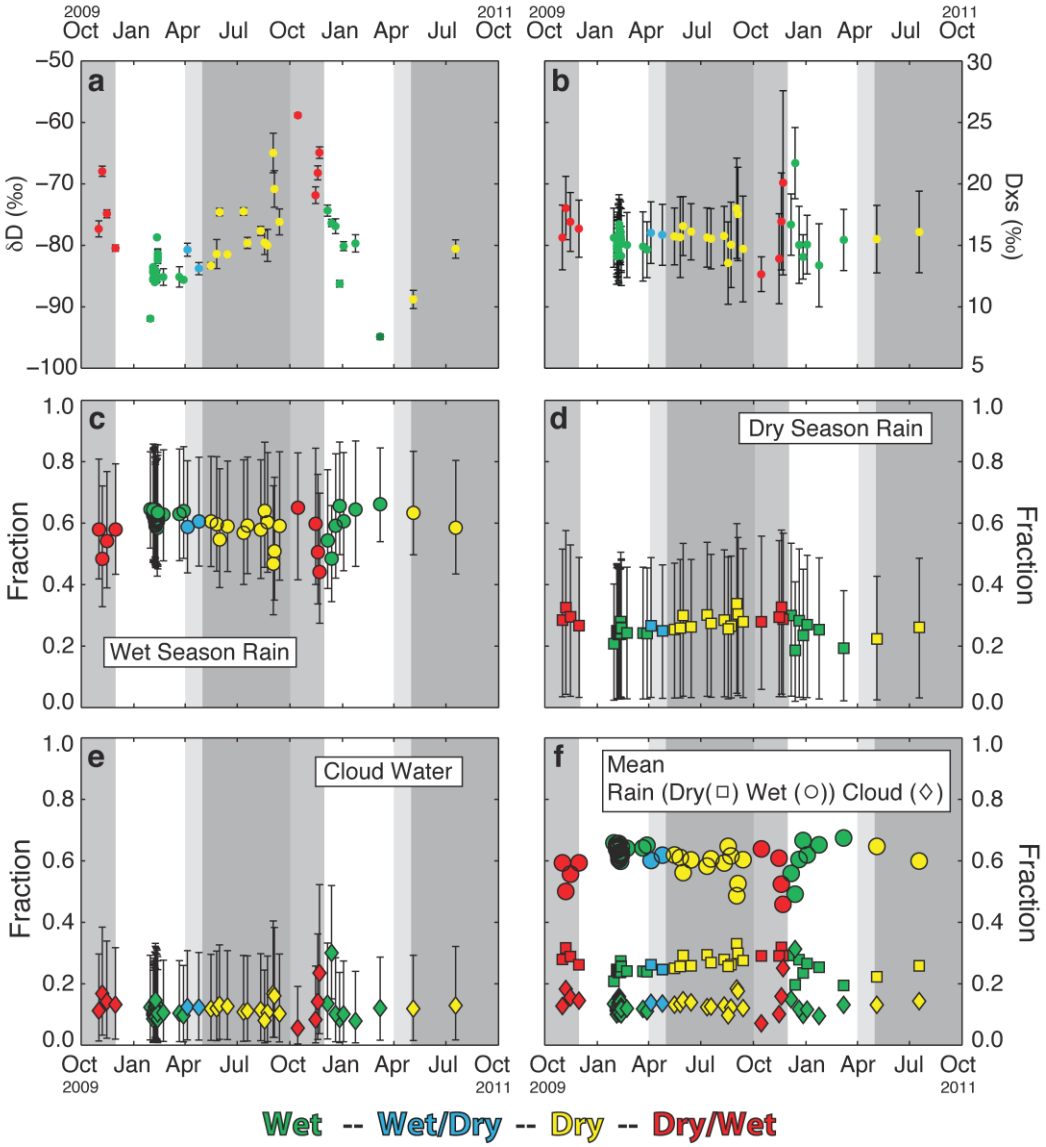

Figure 6: Time series of river water hydrogen isotopes (δD_{river}) and river water deuterium excess (Dxs_{river}), and the calculated mixing proportions of different sources for the Kosñipata River. a) The time series of δD_{river} values with error bars signifying 2 standard deviations. b) The time series of Dxs_{river} values with error bars signifying 2 standard deviations. Time series of the 5th (lower error bar), 50th (open circle), and 95th percentile (upper error bar) values of the distribution of fractional contributions to river discharge, calculated using the three end member mixing model, of: c) wet season rain; d) dry season rain; and e) cloud water vapour. f) Time series of the mean contributions of wet season rain (circle), dry season rain (square), and cloud water vapour (diamond) to river discharge.

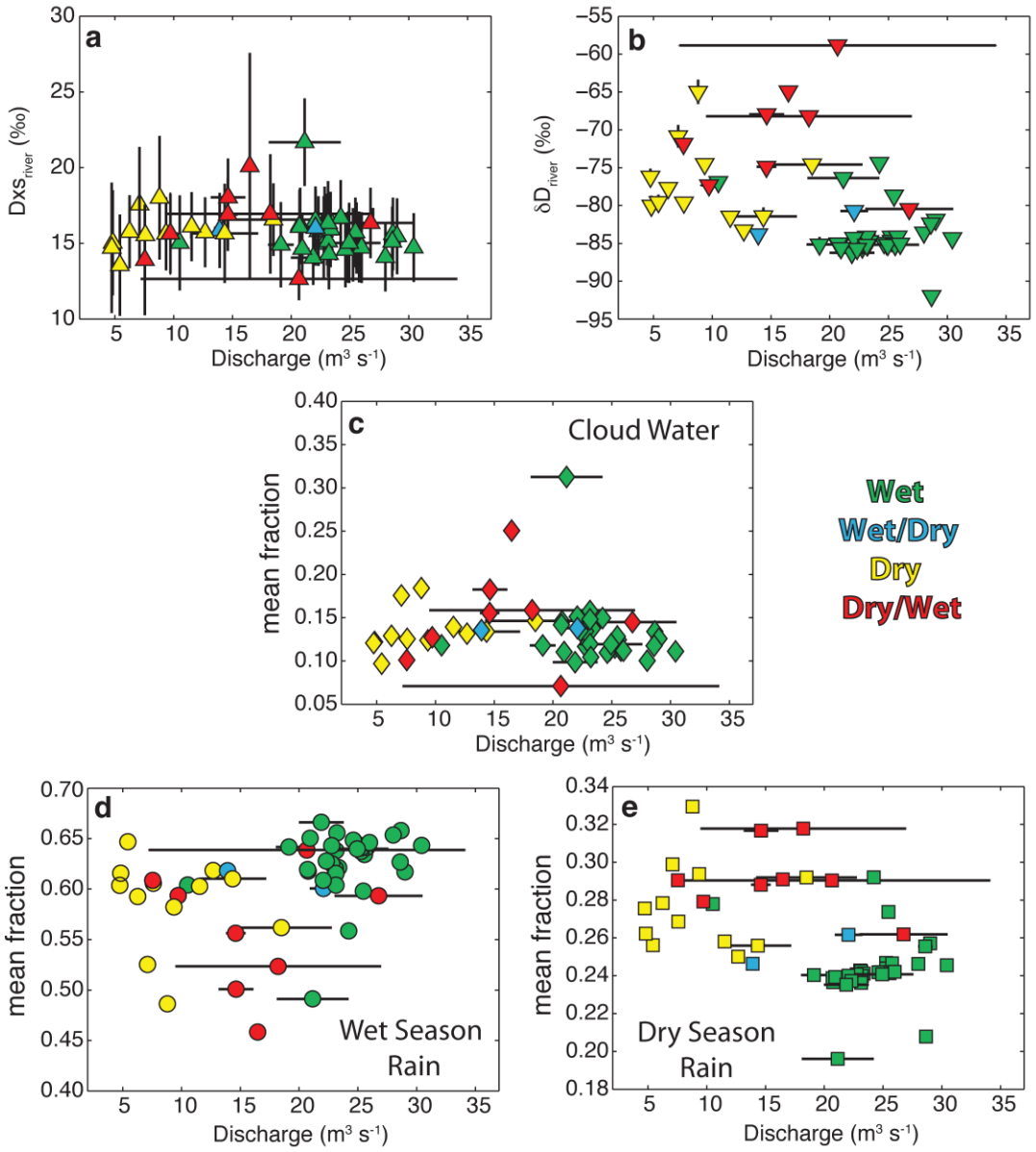

1163

1164 Figure 7: Variation in the isotopic composition of river water a) deuterium excess (Dxs_{river},
1165 %) and b) hydrogen isotope ratio (δD_{river}, ‰) plotted versus discharge ($m^3\ s^{-1}$). Variation in
1166 the mean contributions to river flow as a function of water discharge for cloud water vapour
1167 (c), wet season rain (d), and dry season rain (e) as calculated by the end member mixing
1168 analysis, also plotted versus discharge.

1169

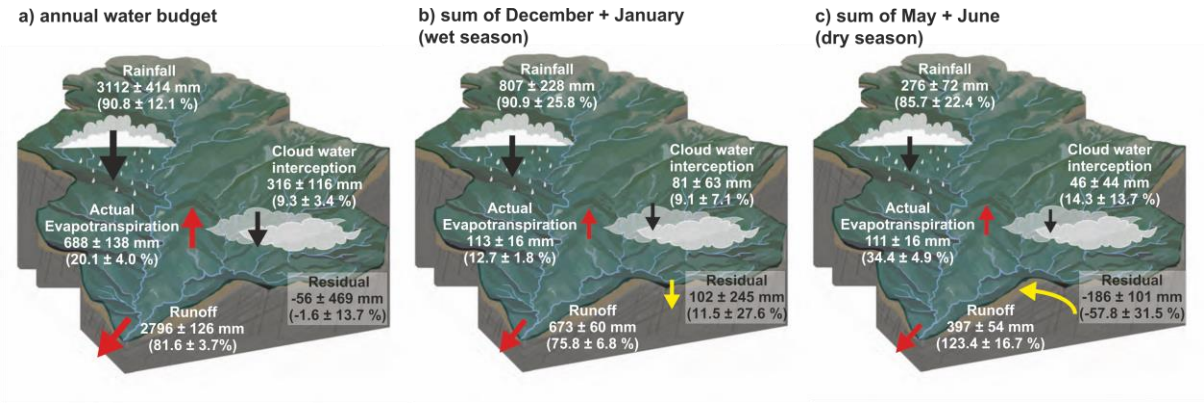

Figure 8: A schematic illustration of the water budget for the Kosñipata catchment for (a) the study year, (b) the early wet season (December and January), and (c) the early dry season (May and June). Black arrows represent inputs and red arrows represent outputs; yellow arrows represent the reversible flux of the residual over the wet and dry seasons, reflecting the transient seasonal storage of water in soil and fractured bedrock (see Discussion in text). The sizes of the arrows are scaled logarithmically with the magnitude of the flux. Values indicated are sums for that time period in mm.

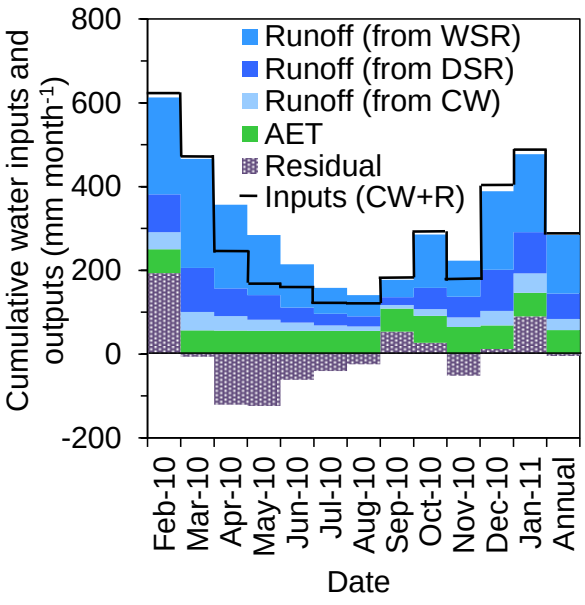

Figure 9: Cumulative water inputs (rainfall and cloud water interception) are represented by the black line. Cumulative water outputs (river runoff and actual evapotranspiration) and the residual are separated out into cumulative coloured stacked bars. Runoff is separated into its 3 sources: wet season rainfall (WSR), dry season rainfall (DSR), and cloudwater (CW) (Table 3). The study period is separated by month and the monthly balance is determined for the study year, February 2010 to January 2011.

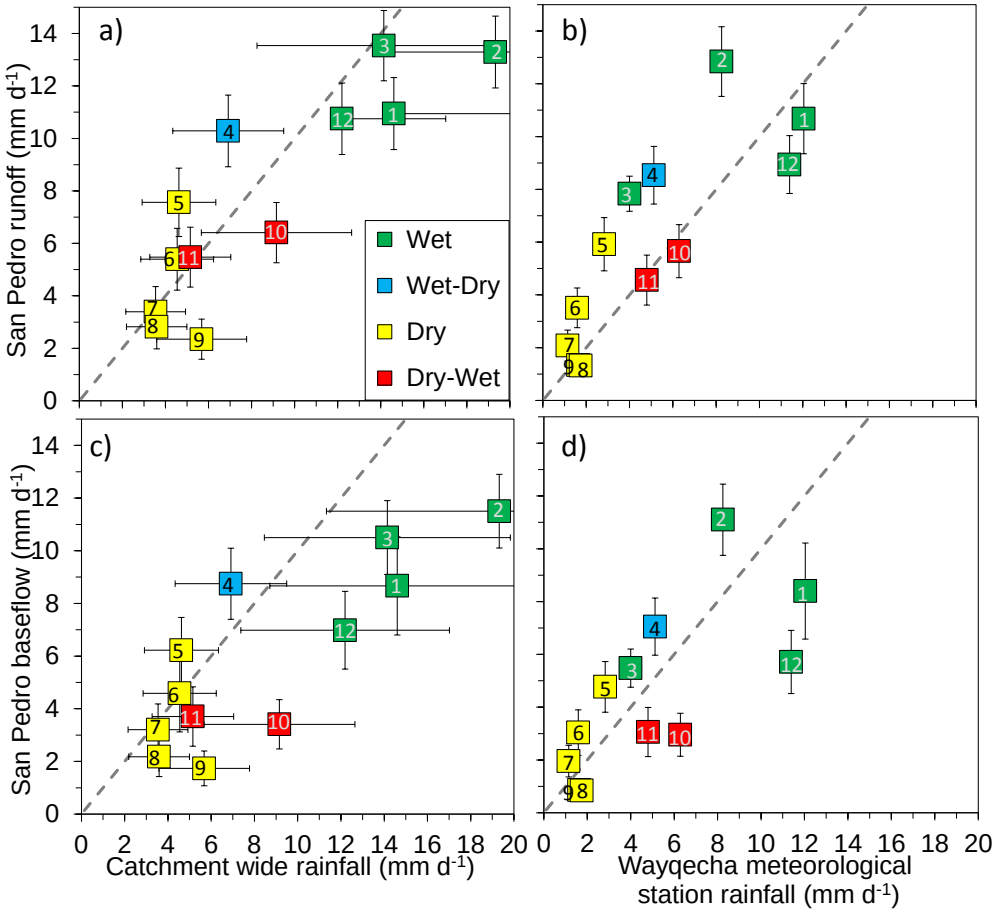

Figure 10: Mean monthly rainfall (corrected for wind-induced loss) versus river runoff (mm d^{-1}) for the Kosñipata catchment, showing anticlockwise hysteresis throughout the year, with months numbered chronologically and colour coded by season (see Figs. 2 & 7). Plots show stream runoff versus a) catchment wide rainfall and b) meteorological station rainfall for the Wayqecha meteorological station (2900 masl), and baseflow versus c) catchment wide rainfall and d) meteorological station rainfall at Wayqecha. Error bars represent one standard deviation. The one-to-one line for rainfall to river runoff is represented by the grey dashed line. Note: in b) and d) days with zero rainfall were excluded as per the approach used by Andermann et al. (2012).